

Scalar perturbations in $f(T)$ gravity using the 1 + 3 covariant approach

Shambel Sahlu^{1,2}, Joseph Ntahompagaze^{1,3}, Amare Abebe⁴, Álvaro de la Cruz-Dombriz⁵, David F. Mota⁶
shambel.sahlu@wku.edu.et

¹ Astronomy and Astrophysics Department, Entoto Observatory and Research Center, Ethiopian Space Science and Technology Institute, Ethiopia

² Department of Physics, College of Natural and Computational Science, Wolkite University, Ethiopia

³ Department of Physics, College of Science and Technology, University of Rwanda, Rwanda

⁴ Center for Space Research, North-West University, Mafikeng, South Africa

⁵ Cosmology and Gravity Group, Mathematics and Applied Mathematics, University of Cape Town, 7701 Rondebosch, South Africa

⁶ Institute of Theoretical Astrophysics, University of Oslo, Oslo, Norway

Abstract

We investigate the cosmological scalar perturbations of standard matter in the context of extended teleparallel $f(T)$ gravity theories using the 1 + 3 covariant formalism. We review the gravitational field equations of $f(T)$ gravity to introduce therein a gauge-invariant spatial gradient of the torsion fluid and obtain the linear perturbation equations. After performing the usual scalar and harmonic decompositions, we analyze the matter perturbations in the quasi-static approximation for two non-interacting fluids scenarios, namely torsion-dust and torsion-radiation mixtures. We consider the $f(T)$ power-law paradigmatic classes of models $f(T) = \alpha T_0 \left(-\frac{T}{T_0}\right)^n$, for both torsion-dust and torsion-radiation scenarios. Under this scope, exact solutions of the matter perturbations are obtained. We examine the growth of the matter density contrast for these mixtures. In a similar manner, we also consider the long- and short-wavelength modes in the torsion-radiation case. We consider different values of n to explore the growth of matter density contrast with red-shift. For the case of n closer to one, our paradigmatic $f(T)$ gravity model is favored with the usual results of general relativity (GR) and general relativity with a cosmological constant (Λ CDM). However, for the case of $n \gg 1$ the amplitude of the matter density fluctuation extremely high and unrealistic to compare with GR and Λ CDM results for these non-interacting fluids. Notably, in the torsion-radiation system, the behavior of the growth of matter density contrasts is abandoned and ruled-out for $n \ll 1$ in both wave modes. While our results show a richer set of possibilities that can help to constrain the model parameters using future observational data, they also accommodate currently known features of power spectrum in the large-scale structure in the general relativistic limit.

PACS numbers 04.50.Kd, 98.80.Jk, 98.80.-k, 95.36.+x, 98.80.Cq

keywords: Teleparallel gravity; 1+3 covariant decomposition; cosmological perturbations; density contrast

1 Introduction

The recent discovery of the accelerating expansion of the Universe [1, 2] has put a big question mark on the General Relativity (GR)-based cosmology. Moreover, there are many outstanding open problems and active theoretical and observational research areas in physical cosmology such as the origin, evolution and formation of the primordial Universe [3, 4, 5, 6], the anisotropy of the Cosmic Microwave Background radiation (CMB) [7, 8, 9], the accelerating expansion of the entire Universe, how cosmological perturbations [10, 11, 12, 13, 14] and the primordial fluctuations of the early Universe formed the large-scale structure [7, 8, 11, 15], and the formation and evolution of the early type astrophysical objects like galaxies [16, 17, 18], to mention but a few. The current Concordance (Λ CDM) cosmological model takes into account the assumption that the Universe passed through different epochs such as inflation, radiation-dominated, matter-dominated and dark energy-dominated epochs. The growth of energy density fluctuations is the cause behind the inhomogeneity and formation of the large-scale structures in the Universe [19]. Of course, different aspects of cosmology can be explored in different extended theories of gravity including $f(T)$ gravity theory [20, 21, 22, 23, 24, 25, 26, 27, 28, 29]. The study of linear cosmological perturbations in $f(T)$ gravity theory using the 1 + 3 covariant formalism is the main issue in this manuscript. Basically, there are two mainstream formalisms to study cosmological perturbations,

namely, the metric formalism [12, 30, 31] and the 1 + 3 covariant gauge-invariant formalism [10, 32, 33, 34, 35], for GR and extended gravity approaches. In the 1 + 3 covariant formalism, the perturbations defined describe true physical degrees of freedom and no physical gauge modes exist. In recent years, there has been active research on cosmological perturbations theory for both GR [36, 37, 38, 39] and different extended gravity theories [32, 33, 40] using the 1 + 3 covariant formalism where the recent observations constrained considered gravity models.

Within the $f(T)$ gravity framework, we will resort to the energy-momentum tensor (EMT) of the torsion [fluid] in addition to the EMT of the physical standard matter fluids [41, 42] to derive the perturbation equations. After deriving the perturbation evolution equations for generic $f(T)$ theories, we will consider the power-law [43, 44, 45] $f(T) = T_0 (-T/T_0)^n$ paradigmatic model admitting an ansatz scale factor of the field equation for matter dominated Universe [46] as $a = a_0 (t/t_0)^m$, for further analysis using the well-known approximation technique dubbed quasi-static approximation [21, 33, 47, 48, 49]. For instance, in [21] the validation of such an approximation technique was considered to explore the so-called effective field theory approach to torsional modified gravities by considering the $k^2/a^2 H^2 \gg 1$ mode.

In this paper, we shall apply this approximation method and assume very slow temporal fluctuations in the perturbations of both the torsion energy density and momentum compared with the fluctuations of matter energy density. As such, the time derivative terms of the fluctuations of torsion density and momentum are neglected. Finally, for comparison, we depict that the growth of the energy density fluctuations with red-shift for both GR and $f(T)$ gravity approaches. The energy density contrasts have done for GR approach in dust-dominated and radiation-dominated Universe, and for $f(T)$ gravity approach in torsion-dust and torsion-radiation systems for both modes, namely short- and long-wavelength modes.

The road-map of this paper is as follows: in the following section, we review the 1 + 3 covariant gauge-invariant cosmological perturbations formalism within the $f(T)$ gravity framework. The kinematic feature of the Universe and the general fluid description are studied in the presence of an effective torsion fluid in Secs. 3 and 4 respectively. In Section 5, we derive the linear evolution equations for matter and torsion perturbations, the scalar decomposition of which will be carried out in Section 6. In Section 7, we discuss the harmonic decomposition of the scalar perturbations and figure out how to analyze the growth of the matter energy density perturbations. We explore the growth of energy density fluctuations in Sec. 8 for dust and radiation fluids in the GR context and in Sec. 9, for the torsion-dust and torsion-radiation systems for $f(T)$ gravity approach. The growth of the energy density contrast $f(T)$ and GR is covered in this section. Finally, we wrap up with the main results of the manuscript in Section 10.

2 The 1 + 3 covariant formalism in $f(T)$ gravity

In the 1 + 3 covariant decomposition formalism, it is assumed that a fundamental observer slices space-time into temporal and spacial hyper-surfaces [50]. Given the fact that the matter components in the Universe would define a physically motivated preferred motion, it is usual to choose the CMB frame, where the radiation dipole vanishes, as the natural reference frame in Cosmology [51, 52]. For the unperturbed (background) Universe, we define the tangent space-time by the tetrad field $e_0^a = u^a$, where u^a is the four-velocity vector of the observer. The preferred world-line is given in terms of local coordinates x^a in the general coordinates $x^a = x^a(\tau)$ and we define the four-vector velocity u^a as

$$u^a = \frac{dx^a}{d\tau}, \quad (1)$$

where τ is measured along the fundamental world-line. According to the reason above, the component of any vector X^a parallel to the 4-velocity vector u^a becomes

$$X^a = U_b^a X^b, \quad U_b^a := -u^a u_b, \quad (2)$$

where U_b^a is the projection tensor into the one-dimensional tangent line and satisfies the following relations:

$$\begin{aligned} U_b^a U_c^b &= U_c^a \implies U_b^a u^a = u^a, \\ u^a &= \delta_0^a \implies U_b^a = \delta_0^a \delta_b^0. \end{aligned} \quad (3)$$

Moreover, we define h_{ab} as another projection tensor into the three-dimensional, orthogonal to u^μ and it

satisfies the following properties:

$$\begin{aligned} h_{ab} &= g_{ab} + u_a u_b \implies h_b^a h_c^b = h_c^a, \\ h_a^a &= 3, \quad h_{ab} u^b = 0. \end{aligned} \quad (4)$$

The action of modified teleparallel gravity (TG) one is given by [44]

$$S_{f(T)} = \frac{1}{2\kappa^2} \int d^4x e [f(T) + 2\mathcal{L}_m], \quad (5)$$

where e is the determinant of the tetrad field e_μ^a i.e., ($e = \det|e_\mu^a| = \sqrt{-g}$) and the coupling constant $\kappa^2 = 8\pi G/c^4$ ¹. Note that, TG and GR could be recover for the limiting case of $f(T) = T$, whereas, we restore GR with cosmological constant so-called Λ CDM for the case of $f(T) = T + 2\Lambda$ [29]. The field equations for $f(T)$ gravity [53] yield

$$G_{ab} = -\frac{1}{2f'} g_{ab} (f - f'T) + \frac{1}{f'} (f'' S_{ab}{}^d \nabla_d T) + \frac{\kappa^2}{f'} \Theta_{ab}^{(m)}, \quad (6)$$

where g_{ab} is the metric, $f' \equiv df/dT$, $f'' \equiv d^2f/dT^2$, $\Theta^{(m)a}{}_b \equiv \frac{1}{e} \frac{\delta(\mathcal{L}_m)}{\delta e_b^a}$ denotes the usual EMT of standard matter (m) fields, and $S_{ab}{}^d$ denotes a *super-potential* term [22, 23, 24]

$$S_{ab}{}^d = \frac{1}{2} (K_{ab}{}^d + \delta_a^d T_{cb}{}^c - \delta_b^d T_{ca}{}^c), \quad (7)$$

where $K_{ab}{}^d$ is the contortion tensor and $T_{cb}{}^c$ is the torsion tensor. It is straightforward to see that the above field equations can be written in the more compact form as

$$G_{ab} = \Theta_{ab}^{(T)} + \Theta_{ab}^{(m)} = \Theta_{ab}^{eff}, \quad (8)$$

where we have defined the EMT of the torsion (T) fluid as [20]

$$\begin{aligned} \Theta_{ab}^{(T)} &= -\frac{1}{2f'} g_{ab} (f - f'T) - \frac{1}{f'} (f'' S_{ab}{}^d \nabla_d T) \\ &\quad - \frac{1}{f'} (f' - 1) \Theta_{ab}^{(m)}. \end{aligned} \quad (9)$$

All thermodynamic quantities, such as the total energy density ρ , isotropic pressure p , heat flux q_a and anisotropic stress tensor π_{ab} for matter (m) and torsion (T) fluids are extracted from the total EMT Θ_{ab} as follows:

$$\rho = \Theta_{ab} u^a u^b, \quad (10)$$

$$p = -\frac{1}{3} h^{ab} \Theta_{ab}, \quad (11)$$

$$q_a = h_a^b u^c \Theta_{bc}, \quad (12)$$

$$\pi_{ab} = h_a^c h_b^d \Theta_{cd} + p h_{ab}, \quad (13)$$

whereas the respective quantities for both matter and torsion components can similarly be extracted from their corresponding EMTs, such that

$$\begin{aligned} \rho &= \rho_T + \rho_m, & p &= p_T + p_m, \\ q^a &= q_T^a + q_m^a, & \pi^{ab} &= \pi_T^{ab} + \pi_m^{ab}. \end{aligned}$$

From Eq. (6), the Friedmann equations of the effective fluid are presented in [20, 53] as follows:

$$H^2 = \frac{\rho_m}{3f'} - \frac{1}{6f'} (f - T f'), \quad (14)$$

$$2\dot{H} + 3H^2 = \frac{p_m}{f'} + \frac{1}{2f'} (f - T f') + \frac{4f'' H \dot{T}}{f'}, \quad (15)$$

¹From here onwards, the geometric units convention where $8\pi G = c = 1$.

where $H(t) \equiv \dot{a}(t)/a(t)$ is the Hubble parameter defined in terms of the scale factor $a(t)$ and its time derivative. One can directly obtain the corresponding thermodynamic quantities such as the effective energy density of the fluid

$$\rho = \frac{\rho_m}{f'} - \frac{1}{2f'}(f - Tf'), \quad (16)$$

and the effective pressure of the fluid

$$p = \frac{p_m}{f'} + \frac{1}{2f'}(f - Tf') + \frac{2f''H\dot{T}}{f'}, \quad (17)$$

respectively. It is easy to show that the Friedmann equations (14)-(15) can be re-expressed as

$$1 = \Omega_m + \mathcal{X}, \quad (18)$$

$$\frac{\dot{H}}{H^2} = -\frac{3}{2} + \frac{\Omega_m}{2} + \frac{3}{2}\mathcal{X} + 3\mathcal{Y}, \quad (19)$$

where we have introduced the following new variables:

$$\mathcal{X} \equiv \frac{Tf' - f}{6H^2f'}, \Omega_m \equiv \frac{\rho_m}{3H^2f'}, \mathcal{Y} \equiv \frac{2\dot{T}f''}{3Hf'}. \quad (20)$$

It is worth noting here that if Ω_d and Ω_r are the fractional energy densities of the dust (d) and radiation (r) fluids respectively, then $\Omega_m = \Omega_d + \Omega_r$. From the above extracted basic quantities, namely the energy density ρ and pressure p of the fluid, in the following we shall investigate the growth of energy density linear perturbations in 1+3 gauge-invariant approach in both the matter and radiation-dominated cosmological epochs. For perfect fluids, the energy flux (12) and the anisotropic stress (13) are identically zero.

In this paper, we consider the non-interacting perfect fluids and the energy flux and anisotropic stress zero in our case. Obviously, in the case of a gravitational Lagrangian $f(T) \equiv T$ [41, 54], the physical quantities in Eqs. (9), (16) and (17) reduce to the usual GR limit. In such a limit, the linear cosmological perturbations have been widely studied in [55, 56].

3 Kinematic quantities in the presence of torsion

As stated previously, the kinematics of the four-velocity vector u^a determines the geometry of the fluid flow. Any tensor V_{ab} can be expressed as a sum of its symmetric $V_{(ab)}$ and anti-symmetric $V_{[ab]}$ parts as

$$V_{ab} = V_{(ab)} + V_{[ab]}. \quad (21)$$

In this formalism, the covariant derivative of u_b is split into the kinematic quantities [57] as

$$\tilde{\nabla}_a u_b = \frac{1}{3}h_{ab}\tilde{\theta} + \tilde{\sigma}_{ab} + \tilde{\omega}_{ab} - u_a\tilde{u}_b, \quad (22)$$

where $\tilde{\theta}$ is the fluid expansion, $\tilde{\sigma}_{ab}$ is the shear tensor, \tilde{u}_a is the four-acceleration of the fluid and $\tilde{\omega}_{ab}$ is the vorticity tensor in the presence of torsion. Notice that a tilde represents torsion-dependent physical parameters and a non-tilde represents Levi-Civita connection-dependent parameters. The detailed expressions of torsion dependent kinematic quantities such as expansion of the fluid, shear tensor, the vorticity tensor and the relativistic acceleration vector are presented in Refs. [25, 26, 27]. The expansion of the fluid flow in the presence of torsion is given by

$$\tilde{\theta} = \theta - 2u^b T_b, \quad (23)$$

where the vector torsion T_b can be either space-like, time-like or light-like and this three different types of vector torsion is discussed in [25]. Here we have defined the Hubble expansion parameter $3H \equiv \theta$ and $\theta = u^b{}_{;b}$ is the volume-expansion. The shear tensor denotes the change of distortion of the matter flow with time and it is given as

$$\tilde{\sigma}_{ab} = \sigma_{ab} + 2h_a^c h_b^d K_{[cd]}^e u_e, \quad (24)$$

and the vorticity tensor denotes the rotation of the matter relative to the non-rotating (Fermi-propagated) frame and it is given as

$$\tilde{\omega}_{ab} = \omega_{ab} + 2h_a^c h_b^d K_{[cd]}^e u_e. \quad (25)$$

Also, the relativistic acceleration vector describes the degree of matter to move under forces other than gravity plus inertia, namely

$$\dot{u}_a = \dot{u}_a + u^b K_{ab}^e u_e, \quad (26)$$

which vanishes for free-falling matter. The general expression for the torsion-based Raychaudhuri equation is given by [25, 26, 27]

$$\begin{aligned} \dot{\theta} = & \tilde{\nabla}^a \dot{u}_a - \frac{1}{3} \theta^2 - \tilde{\sigma}^{cb} \tilde{\sigma}_{cb} - \tilde{\omega}^{cb} \tilde{\omega}_{cb} - R_{cb} u^c u^b \\ & - 2u^b T_{cb}^d \left(\frac{1}{3} h_d^c \tilde{\theta} - \tilde{\sigma}_d^c - \tilde{\omega}_d^c - u^c \dot{u}_d \right). \end{aligned} \quad (27)$$

In this paper, we assume that the world-line is tangent to u^c but parallel to \dot{u}_c , i.e., $u^c \dot{u}_c = 0$. Moreover, $\tilde{\omega}_{cb} = 0 = \tilde{\sigma}_{cb}$ in the case of non-rotational and shear-free fluids and from the covariant approach of the field equation, $R_{cb} u^c u^b = 1/2 (\rho + 3p)$ for relativistic fluid [58, 59]. Then, Eq. (27) becomes

$$\dot{\theta} = \tilde{\nabla}^a \dot{u}_a - \frac{1}{3} \theta^2 - \frac{1}{2} (\rho + 3p) - \frac{2}{3} u^b T_b \tilde{\theta}. \quad (28)$$

For a space-like torsion vector the inner product of the torsion and four-velocity vectors of the fluid $u^b T_b$ is vanished identically [27].

Consequently, Eq. (23) reads $\tilde{\theta} = \theta$ and Eq. (26) reads $\dot{u}_a = \dot{u}_a$. Then, from the result of Eq. (28), we obtain

$$\dot{\theta} = -\frac{\theta^2}{3} - \frac{1}{2} (\rho + 3p) + \tilde{\nabla}^a \dot{u}_a, \quad (29)$$

and this equation is the same as the usual Raychaudhuri equation which is presented in Refs. [38, 41, 58, 60].

4 General fluid description

Here, we assume the non-interacting matter fluid ($\rho_m \equiv \rho_r + \rho_d$) with torsion fluid in the entire Universe and the growth of the matter energy density fluctuations has a significant role for formation of large-scale structures.

4.1 Matter fluids

Let us consider a homogeneous and isotropic expanding (FLRW) cosmological background and define spatial gradients of gauge-invariant variables such as those of the energy density X_a , pressure Y_a and volume expansion of the fluid Z_a as follows [33, 38, 61, 62]:

$$D_a^m \equiv \frac{a}{\rho_m} \tilde{\nabla}_a \rho_m, \quad (30)$$

$$Z_a \equiv \tilde{\nabla}_a \theta. \quad (31)$$

Those two gradient variables are a key points to examine evolution equation for matter density fluctuations.

4.2 Torsion fluids

Analogously to the 1 + 3 cosmological perturbations treatment for $f(R)$ gravity theory [33], let us define extra key variables resulting from spatial gradients of gauge-invariant quantities which are connected with the torsion fluid for $f(T)$ gravity. Accordingly, we define the quantities \mathcal{F}_a and \mathcal{B}_a as

$$\mathcal{F}_a \equiv a \tilde{\nabla}_a T, \quad (32)$$

$$\mathcal{B}_a \equiv a \tilde{\nabla}_a \dot{T}, \quad (33)$$

to characterize the fluctuations in the torsion density and momentum respectively.

All the quantities listed in Eqs. (30) - (33) will be considered to develop the system of cosmological perturbation equations for $f(T)$ gravities in the 1 + 3 covariant formalism. Moreover, for each non-interacting fluid, the following conservation equations, considered in [37, 38]

$$\dot{\rho}_m = -\theta(\rho_m + p_m) + (\rho_m + p_m)\tilde{\nabla}^a \Psi_a, \quad (34)$$

$$(\rho_m + p_m)\dot{u}_a + \tilde{\nabla}_a p_m + \dot{\Psi}_a - (3c_s^2 - 1)\frac{\theta}{3}\Psi_a + \Pi_a = 0, \quad (35)$$

hold, where

$$\Psi_a = \frac{q_a}{(\rho_m + p_m)}, \quad \Pi_a = \frac{\tilde{\nabla}^b \pi_{ab}}{\rho_m + p_m}. \quad (36)$$

The speed of sound $c_s^2 = \frac{\delta p}{\delta \rho}$ would play an important role since it allows us to relate the perturbed pressure with the energy density of the fluid. Also, the time derivative of equation of state parameter $\dot{w} = \dot{p}_m/\dot{\rho}_m$ can be expressed with speed of sound [33], and the non-constant equation of state parameter for all fluids as

$$\dot{w} = (1 + w)(w - c_s^2), \quad (37)$$

and this equation of state parameter is the generalized one for all matter fluids. In fact, for non-interacting fluids, in the following we shall consider the equation of state parameter to be independent of time, thus $\dot{w} = 0$. In this approach, the speed of sound becomes equivalent to the equation of state parameter $w = c_s^2$ [63]. For perfect fluid the energy flux and anisotropic-stress are zero ($\Psi_a = \Pi_a = 0$).

5 Linear evolution equations

Here we derive the first-order evolution equations for the above-defined gauge-invariant gradient variables. In the energy frame of the matter fluid, these evolution equations for the perturbations are given as:

$$\dot{D}_a^m = -(1 + w)Z_a + w\theta D_a^m, \quad (38)$$

$$\begin{aligned} \dot{Z}_a = & \left[\frac{w\theta^2}{3(1+w)} - \frac{1+3w}{2f'(1+w)}\rho_m - \frac{w}{2f'(1+w)}(f - Tf') - \frac{2f''w}{3f'(1+w)}\theta\dot{T} - \frac{w}{1+w}\tilde{\nabla}^2 \right] D_a^m \\ & + \left[\frac{2f''}{3f'}\dot{T} - \frac{2\theta}{3} \right] Z_a - \left[\frac{3\rho_m f''}{2f'^2} + \frac{3w\rho_m f''}{2f'^2} + \frac{2f''^2}{3f'^2}\theta\dot{T} - \frac{2f'''\theta\dot{T}}{3f'} \right] \mathcal{F}_a + \frac{2f''\theta}{3f'} \mathcal{B}_a, \end{aligned} \quad (39)$$

$$\dot{\mathcal{F}}_a = \mathcal{B}_a - \frac{w\dot{T}}{1+w}D_a^m, \quad (40)$$

$$\dot{\mathcal{B}}_a = \frac{\ddot{T}}{\dot{T}}\mathcal{F}_a - \frac{w\ddot{T}}{1+w}D_a^m. \quad (41)$$

In the following section, we will see how to decompose the evolution of the above vector gradient variables (38) - (41) into those of scalar variables by applying the scalar decomposition method outlined.

6 Scalar decomposition

It is generally understood that the large-scale structure formation follows a spherical clustering mechanism, and that only the scalar (non-solenoidal) parts of the above gradient vectors (38) - (41) assist in the clustering. As a result, we extract the scalar part of a vector \mathcal{I}_a by taking its divergence as [33]

$$a\tilde{\nabla}_a \mathcal{I}_b = \mathcal{I}_{ab} = \frac{1}{3}h_{ab}\mathcal{I} + \Sigma \frac{\mathcal{I}}{ab} + \mathcal{I}_{[ab]}, \quad (42)$$

where

$$\mathcal{I} = \tilde{\nabla}_a \mathcal{I}^a, \quad \text{and} \quad \Sigma \frac{\mathcal{I}}{ab} = \mathcal{I}_{(ab)} - \frac{1}{3}h_{ab}\mathcal{I}. \quad (43)$$

The last two terms of Eq. (42) describe shear and vorticity effects, respectively. To extract the (scalar) density contrast, the vorticity vanishes and only the shear part is considered. From vector quantities, one can further

extract the scalar gradient quantities of our cosmological perturbations, believed to be responsible for the spherical clustering of large-scale structure [33, 64]. Let us now define our scalar gradient variables as follows:

$$\Delta_m = a\tilde{\nabla}^a D_a^m, \quad (44)$$

$$Z = a\tilde{\nabla}^a Z_a, \quad (45)$$

$$\mathcal{F} = a\tilde{\nabla}^a \mathcal{F}_a, \quad (46)$$

$$\mathcal{B} = a\tilde{\nabla}^a \mathcal{B}_a. \quad (47)$$

It can be shown that these quantities evolve as:

$$\dot{\Delta}_m = -(1+w)Z + w\theta\Delta_m, \quad (48)$$

$$\begin{aligned} \dot{Z} = & \left[\frac{w\theta^2}{3(1+w)} - \frac{1+3w}{2f'(1+w)}\rho_m - \frac{w}{2f'(1+w)}(f - Tf') - \frac{2f''w}{3f'(1+w)}\theta\dot{T} - \frac{w}{1+w}\tilde{\nabla}^2 \right] \Delta_m \\ & + \left[\frac{2f''}{3f'}\dot{T} - \frac{2\theta}{3} \right] Z - \left[\frac{3\rho_m f''}{2f'^2} + \frac{3w\rho_m f''}{2f'^2} + \frac{2f''^2}{3f'^2}\theta\dot{T} - \frac{2f'''}{3f'}\theta\dot{T} \right] \mathcal{F} + \frac{2f''\theta}{3f'}\mathcal{B}, \end{aligned} \quad (49)$$

$$\dot{\mathcal{F}} = \mathcal{B} - \frac{w\dot{T}}{1+w}\Delta_m, \quad (50)$$

$$\dot{\mathcal{B}} = \frac{\ddot{T}}{\dot{T}}\mathcal{F} - \frac{w\ddot{T}}{1+w}\Delta_m. \quad (51)$$

Finally, the second-order scalar evolution equations can be derived by differentiating the above first-order evolution equations with respect to time. For instance, from Eqs. (48) and (49) we obtain

$$\begin{aligned} \ddot{\Delta}_m = & \left[\frac{1+3w}{2f'}(1-w)\rho_m + \frac{w}{f'}(f - Tf') - \frac{2f''w}{3f'}\theta\dot{T} + w\tilde{\nabla}^2 \right] \Delta_m \\ & + \left[\frac{f''}{3f'}\dot{T} + \theta \left(w - \frac{2}{3} \right) \right] \dot{\Delta}_m + \left[\frac{3\rho_m f''}{2f'^2} + \frac{3w\rho_m f''}{2f'^2} + \frac{2f''^2}{3f'^2}\theta\dot{T} - \frac{2f'''}{3f'}\theta\dot{T} \right] (1+w)\mathcal{F} - \frac{2f''}{3f'}\theta(1+w)\dot{\mathcal{F}} \end{aligned} \quad (52)$$

whereas from Eqs. (50) and (51) we get

$$\ddot{\mathcal{F}} = \frac{\ddot{T}}{\dot{T}}\mathcal{F} - \frac{2w\ddot{T}}{1+w}\Delta_m - \frac{w\dot{T}}{1+w}\dot{\Delta}_m. \quad (53)$$

The scalar gradient variables (38) - (53) we take as an input to study the energy density fluctuations in different cosmological era by applying the harmonic decomposition of these variables in the next section.

7 Harmonic decomposition of variables

From the results of the previous section, we clearly see that the linear cosmological evolution equations of the scalar variables are second-order differential equations, complicated to solve. Thus, in order to obtain the eigenfunctions and the corresponding wave-numbers from those second-order differential equations, we shall apply the separation-of-variables technique. Then we shall use the standard harmonic decomposition of the evolution equations for cosmological perturbations [33, 61, 65] for further details on this technique). All the above linear evolution equations (48) - (53) have a similar structure as the harmonic oscillator equation and the second-order differential evolution equations for any functions X and Y can be represented schematically as [33]

$$\ddot{X} = A\dot{X} + BX - C(Y, \dot{Y}), \quad (54)$$

where the terms A , B , and C represent the damping oscillator or frictional force, restoring force and source force respectively. Then by applying the separation-of-variables technique, we express

$$X = \sum_k X^k(t)Q^k(\vec{x}), \quad \text{and} \quad Y = \sum_k Y^k(t)Q^k(\vec{x}), \quad (55)$$

where k is the wave-number and $Q^k(x)$ is the eigenfunctions of the covariant derivative. The wave-number k represent the order of the harmonic oscillator and relate with the scale factor as $k = \frac{2\pi a}{\lambda}$, where λ is the

wavelength of the perturbations. Here, we define eigenfunctions of the covariant derivative with the Laplace-Beltrami operator for FLRW space-time as

$$\tilde{\nabla}^2 Q^k(x) = -\frac{k^2}{a^2} Q^k(x). \quad (56)$$

Armed with all this machinery, the first and second-order evolution equations (48) - (53) are expressed as:

$$\dot{\Delta}_m^k = -(1+w)Z_m^k + w\theta\Delta_m^k, \quad (57)$$

$$\begin{aligned} \dot{Z}^k = & \left[\frac{w\theta^2}{3(1+w)} - \frac{1+3w}{2f'(1+w)}\rho_m - \frac{w}{2f'(1+w)}(f - Tf') - \frac{2f''w}{3f'(1+w)}\theta\dot{T} + \frac{wk^2}{a^2(1+w)} \right] \Delta_m^k \\ & + \left[\frac{2f''}{3f'}\dot{T} - \frac{2\theta}{3} \right] Z - \left[(1+w)\frac{3\rho_m f''}{2f'^2} + \frac{2f''^2}{3f'^2}\theta\dot{T} - \frac{2f'''}{3f'}\theta\dot{T} \right] \mathcal{F}^k + \frac{2f''\theta}{3f'} \mathcal{B}^k, \end{aligned} \quad (58)$$

$$\dot{\mathcal{F}}^k = \mathcal{B}^k - \frac{w\dot{T}}{1+w}\Delta_m^k, \quad (59)$$

$$\dot{\mathcal{B}}^k = \frac{\ddot{T}}{\dot{T}}\mathcal{F}^k - \frac{w\ddot{T}}{1+w}\Delta_m^k, \quad (60)$$

$$\begin{aligned} \ddot{\Delta}_m^k = & \left[\frac{1+3w}{2f'}(1-w)\rho_m + \frac{w}{f'}(f - Tf') - \frac{2f''w}{3f'}\theta\dot{T} - \frac{wk^2}{a^3} \right] \Delta_m^k + \left[\frac{f''}{3f'}\dot{T} + \theta \left(w - \frac{2}{3} \right) \right] \dot{\Delta}_m^k \\ & + \left[(1+w)\frac{3\rho_m f''}{2f'^2} + \frac{2f''^2}{3f'^2}\theta\dot{T} - \frac{2f'''}{3f'}\theta\dot{T} \right] (1+w)\mathcal{F}^k - \frac{2f''}{3f'}\theta(1+w)\dot{\mathcal{F}}^k, \end{aligned} \quad (61)$$

$$\ddot{\mathcal{F}}^k = \frac{\ddot{T}}{\dot{T}}\mathcal{F}^k - \frac{2w\ddot{T}}{1+w}\Delta_m^k - \frac{w\dot{T}}{1+w}\dot{\Delta}_m^k. \quad (62)$$

In the following, we shall apply the aforementioned quasi-static approximation in which time fluctuations in the perturbations of the torsion energy density \mathcal{F}^k and momentum \mathcal{B}^k are assumed to be constant with time, i.e., one is allowed to take $\dot{\mathcal{F}}^k = \ddot{\mathcal{F}}^k = \dot{\mathcal{B}}^k \approx 0$. Under this approximation, the first-order linear evolution equations (57)-(58) reduce to:

$$\dot{\Delta}_m^k = -(1+w)Z_m^k + w\theta\Delta_m^k, \quad (63)$$

$$\begin{aligned} \dot{Z}^k = & \left[\frac{w\theta^2}{3(1+w)} - \frac{1+3w}{2f'(1+w)}\rho_m - \frac{w}{2f'(1+w)}(f - Tf') + \frac{wk^2}{a^2(1+w)} \right] \Delta_m^k + \left(\frac{2f''}{3f'}\dot{T} - \frac{2\theta}{3} \right) Z \\ & - \left(\frac{3\rho_m f''}{2f'^2} + \frac{3w\rho_m f''}{2f'^2} + \frac{2f''^2}{3f'^2}\theta\dot{T} - \frac{2f'''}{3f'}\theta\dot{T} \right) \mathcal{F}^k. \end{aligned} \quad (64)$$

Also, from Eqs. (59) and (62) results the relation

$$\mathcal{F}^k = \frac{2w\dot{T}\ddot{T}}{(1+w)\dot{T}^3}\Delta_m^k + \frac{w\dot{T}^2}{(1+w)\dot{T}^3}\dot{\Delta}_m^k. \quad (65)$$

By using the latter Eq. (65) together with the quasi-static approximation itself, Eq. (61) for matter energy density perturbations yields

$$\begin{aligned} \ddot{\Delta}_m^k = & \left\{ \frac{1+3w}{2f'}(1-w)\rho_m + \frac{w}{f'}(f - Tf') - \frac{2f''w}{3f'}\theta\dot{T} - w\frac{k^2}{a^2} + (1+w) \left[\frac{3\rho_m f''}{2f'^2} + \frac{2f''^2}{3f'^2}\theta\dot{T} \right. \right. \\ & \left. \left. - \frac{2f'''}{3f'}\theta\dot{T} \right] \frac{2w\dot{T}\ddot{T}}{\dot{T}^3} \right\} \Delta_m^k + \left[\frac{f''}{3f'}\dot{T} + \theta \left(w - \frac{2}{3} \right) + \left(\frac{3\rho_m f''}{2f'^2} + \frac{3w\rho_m f''}{2f'^2} + \frac{2f''^2}{3f'^2}\theta\dot{T} - \frac{2f'''}{3f'}\theta\dot{T} \right) \frac{w\dot{T}^2}{\dot{T}^3} \right] \dot{\Delta}_m^k \end{aligned} \quad (66)$$

For the case of $f(T) = T + 2\Lambda$, Eq. (66) is reduced to the well-known evolution equation of Λ CDM:

$$\begin{aligned} \ddot{\Delta}_m^k = & \left[\frac{3}{2}\Omega_m(1+3w)(1-w)H^2 + 6wH^2\Omega_\Lambda - w\frac{k^2}{a^2} \right] \Delta_m^k \\ & + 3H \left(w - \frac{2}{3} \right) \dot{\Delta}_m^k, \end{aligned} \quad (67)$$

where the energy density of cosmological constant fluid $\Lambda = 3H_0^2\Omega_\Lambda$. In this context, the matter and cosmological constant fluids have involved in the growth of the energy density fluctuations and formation of large-scale structures. Also, for the paradigmatic case of $f(T) = T$ [41] GR is exactly recovered and the evolution equation (66) coincides with GR as [32]

$$\begin{aligned} \ddot{\Delta}_m^k &= \left[\frac{3}{2}\Omega_m(1+3w)(1-w)H^2 - w\frac{k^2}{a^2} \right] \Delta_m^k \\ &+ 3H \left(w - \frac{2}{3} \right) \dot{\Delta}_m^k . \end{aligned} \quad (68)$$

As we shall see in the following sections, Eq. (66) remains a key equation for analyzing the growth of energy density fluctuations capable of explaining the formation of large-scale structures. For the sake of simplicity and with the aim at illustrating the versatility of our analysis, we shall consider paradigmatic power-law $f(T)$ gravity models

$$f(T) = \alpha T_0 \left(-\frac{T}{T_0} \right)^n , \quad (69)$$

where α and n are dimensionless constants, and $T_0 = -6H_0^2$ is the present-day value of the torsion scalar. We assume the ansatz for the scale factor solution [46, 66, 67]

$$a(t) = a_0(t/t_0)^m , \quad (70)$$

where m is a positive constant, and as usual the scale factor is related to the cosmological red-shift as $a = a_0/(1+z)$ ². For convenience, we also transform any time derivative functions f and H into a red-shift derivative as follows:

$$\frac{\dot{f}}{H} = \frac{df}{dN}, \quad \text{where} \quad N \equiv \ln(a) , \quad (71)$$

$$\dot{f} = -(1+z)H \frac{df}{dz} , \quad (72)$$

$$\ddot{f} = (1+z)^2 H \left(\frac{dH}{dz} \frac{df}{dz} + H \frac{d^2f}{dz^2} \right) , \quad (73)$$

$$\dot{H} = -(1+z)H \frac{dH}{dz} = -\frac{6H^2\mathcal{Y}}{8(n-1)} , \quad (74)$$

$$\frac{dH}{dz} = \frac{6H\mathcal{Y}}{8(1+z)(n-1)} . \quad (75)$$

Before solving the linear evolution equations (63) - (66), let us point out that for $f(T)$ gravity model (69) and scale factor (70), the background quantities \mathcal{X} and \mathcal{Y} as defined in Eq. (20) become

$$\mathcal{Y} = \frac{8(n-1)}{6m} , \quad (76)$$

$$\mathcal{X} = \frac{1-n}{n}, \quad n \neq 0 . \quad (77)$$

From Eq. (18), we redefine the normalized energy density parameter for non-interacting torsion-matter fluids as $1 = \Omega_d + \Omega_T$, i.e. $\Omega_T \equiv \mathcal{X}$ is the normalized energy density parameter of torsion fluid. Consequently, the normalized energy density parameter for matter yields

$$\Omega_m = \frac{2n-1}{n} . \quad (78)$$

For the case of $n < 0.5$, the normalized matter energy density parameter has a negative sign which shows an unphysical mode. Based on relation (78), With this definition, it is possible to know the amount matter fluid in the non-interacting system and analyze the growth of matter fluctuations with red-shift (we will see in detail for torsion-dust and torsion-radiation cases in Sec. 9). As an example: for $n = 1$, the matter fluid is large enough in the system and the torsion fluid becomes negligible. In this case, we obtain the matter dominated

²In this manuscript, both a_0 and t_0 are normalized to unity for simplicity.

Universe and our generalized evolution Eq. (66) reduces to Eq. (68). For $n \geq 1$, $\Omega_m \geq 1$ and $\Omega_T \leq 0$, in this situation the matter fluid is a major component of the Universe and the contributions of torsion like fluid with a negative energy density are the same as of a cosmological constant. However, the effective energy density of the fluid becomes $\rho = \rho_m + \rho_T \geq 0$ [20] as presented in Eq. (16).

Here, we define the normalized energy density contrast for matter fluid as

$$\delta(z) \equiv \frac{\Delta_m^k(z)}{\Delta_{in}}, \quad (79)$$

where the subscript in refers the initial value of $\Delta_m(z)$ at initial red-shift z_{in} ³.

Indeed, the variation of CMB temperature detected observationally is of the order of 10^{-5} [68] and this variation strongly supports the gravitational perturbations initially through their red-shifting effect on the CMB [69, 70]. Also, we shall assume the following initial conditions as $\Delta_{in} \equiv \Delta^k(z_{in} = 1100) = 10^{-5}$ and $\dot{\Delta}_{in} \equiv \dot{\Delta}^k(z_{in} = 1100) = 0$, for every mode k to deal with the growth of matter fluctuations (similar analysis is done in [71]). The energy density fluctuations $\Delta_m(z_{in}) = \Delta_{in} = 10^{-5}$ for all n at the initial red-shift $z_{in} = 1100$. At this red-shift the value of the normalized energy density perturbations of the matter fluid presented in Eq. (79) becomes one ($\delta(z_{in}) = 1$). Moreover, we define the relative difference of matter energy density fluctuations between results for $f(T)$ gravity and GR as

$$\varrho(z) \equiv \frac{|\delta(z) - \delta_{GR}|}{\delta_{GR}}, \quad (80)$$

where analogously to (79)

$$\delta_{GR}^k \equiv \frac{\Delta_m^k(z)(n=1)}{\Delta_i(z_{in})}. \quad (81)$$

For the case of $f(T) \equiv T$, $f(T)$ gravity coincides with TEGR. In this limit, $\delta^k(z) = \delta_{GR}^k$ and $\delta(z)$ can be reduced to the GR limit and $\varrho(z) = 0$.

8 Matter density fluctuations in Λ CDM and GR Limits

In this section, we analyze the growth of the energy density fluctuations for dust and radiation fluids in Λ CDM and GR limits from Eqs. (67) and (68) respectively.

8.1 Dust-dominated Universe

If, we assume that the Universe is dominated by dust fluid only, then the equation of state parameter is $w_d \approx 0$. Consequently, Eq. (67) and Eq. (68) read

$$\ddot{\Delta}_d + 2H\dot{\Delta}_d - \frac{3}{2}\Omega_d H^2 \Delta_d = 0. \quad (82)$$

By applying Eq. (71) this equation becomes

$$\frac{d^2 \Delta_d(z)}{dz^2} - \frac{1}{2(1+z)} \frac{d\Delta_d(z)}{dz} - \frac{2\Omega_d \Delta_d(z)}{3(1+z)^2} = 0. \quad (83)$$

and admits the solution

$$\begin{aligned} \Delta(z) = & C_1(1+z)^{\frac{1}{4}(1+\sqrt{24\Omega_d+9})} \\ & + C_2(1+z)^{\frac{1}{4}(1-\sqrt{24\Omega_d+9})}, \end{aligned} \quad (84)$$

where C_1 and C_2 are integration constants and we determine these constants by imposing the above initial conditions.

³We set the initial conditions at $z_{in} \approx 1100$ during the decoupling era. So, in the following two sections we shall explore the feature of fractional energy density perturbations $\delta(z)$ with red-shift $0 \leq z \leq 1100$.

In the dust-dominated Universe, the input parameter Ω_d is a key point to determine the magnitude of matter fluctuations with red-shift. For instance, the numerical result of Eq. (84) is presented in Fig. 7 (see Appendix 11.1 for $\Omega_d = 1$ and it shows the growth of energy density fluctuations of dust fluid in the dust-dominated Universe⁴. On the other hand, we fill in for the observed value of $\Omega_d = 0.32$ [72] in Eq. (84) to see the effect on the growth of matter density contrast and present the numerical plot in Fig. 8 (see Appendix 11.1. With this plot, the matter density contrasts is also growing up with red-shift.

8.2 Radiation-dominated Universe

8.2.1 For Λ CDM Limit

Here, we study the growth of energy density perturbations of the radiation fluid, by assuming the Universe has two non-interacting cosmic fluid components, namely radiation and the cosmological constant. In this assumption, the equation of state parameter $w_r \approx 1/3$ and the normalized energy density parameter is $\Omega_\Lambda = 1 - \Omega_r$. Then, Eq. (67) in red-shift space becomes

$$\frac{d^2\Delta_r(z)}{dz^2} + \frac{1}{1+z} \frac{d\Delta_r(z)}{dz} - \frac{1}{(1+z)^2} \left[2(\Omega_r + \Omega_\Lambda) - \frac{k^2}{3a^2H^2} \right] \Delta_r(z) = 0. \quad (85)$$

The exact solution for the short-wavelength mode, $k^2/a^2H^2 \gg 1$, becomes

$$\begin{aligned} \Delta_r^k(z) = & C_1 \text{BesselJ} \left(\frac{1}{2} \sqrt{2(\Omega_r + \Omega_\Lambda)}, \frac{2}{3} \frac{\sqrt{3}\pi}{\lambda (1+z)^2} \right) \\ & + C_2 \text{BesselY} \left(\frac{1}{2} \sqrt{2(\Omega_r + \Omega_\Lambda)}, \frac{2}{3} \frac{\sqrt{3}\pi}{\lambda (1+z)^2} \right), \end{aligned} \quad (86)$$

whereas in the long-wavelength mode, $k^2/a^2H^2 \ll 1$, the exact solution reads⁵

$$\Delta(z) = \log(1+z) \left[C_1 \sinh \left(\sqrt{2(\Omega_r + \Omega_\Lambda)} \right) + C_2 \cosh \left(\sqrt{2(\Omega_r + \Omega_\Lambda)} \right) \right]. \quad (87)$$

8.2.2 For GR Limit

For the radiation-dominated Universe, the red-shift dependent of evolution Eq. (68) becomes

$$\frac{d^2\Delta_r(z)}{dz^2} + \left(\frac{1}{1+z} \right) \frac{d\Delta_r(z)}{dz} - \frac{1}{(1+z)^2} \left[2\Omega_r - \frac{16\pi^2}{3\lambda^2(1+z)^4} \right] \Delta_r(z) = 0. \quad (88)$$

The exact solution of Eq. (89) for short-wavelength mode is

$$\begin{aligned} \Delta_r^k(z) = & C_1 \text{BesselJ} \left(\frac{1}{2} \sqrt{2\Omega_r}, \frac{2}{3} \frac{\sqrt{3}\pi}{\lambda (1+z)^2} \right) \\ & + C_2 \text{BesselY} \left(\frac{1}{2} \sqrt{2\Omega_r}, \frac{2}{3} \frac{\sqrt{3}\pi}{\lambda (1+z)^2} \right), \end{aligned} \quad (89)$$

⁴For all figures, we use the black dotted line to shows the energy density fluctuations growth (at $z_0 = 0$) and $\lambda = 0.05 \text{Mpc}$ for plotting in this manuscript.

⁵Note that we have used the relation

$$\frac{k^2}{a^2H^2} = \frac{16\pi^2}{\lambda^2(1+z)^4}.$$

and for long-wavelength mode we have

$$\Delta(z) = \log(1+z) \left[C_1 \sinh\left(\sqrt{2\Omega_r}\right) + C_2 \cosh\left(\sqrt{2\Omega_r}\right) \right]. \quad (90)$$

Notice that, the difference between Λ CDM and GR limits is the parameter Ω_Λ which is not appeared in GR or $\Omega_\Lambda = 0$ in GR solutions⁶. The numerical results of the growth of matter density contrast for Eqs. (86) and (89) and also Eqs. (87) and (90) are depicted in Figs. 10 and 9 respectively (see Appendix 11.1).

The current observational data indicates that the growth of energy density fluctuations of radiation fluid is almost negligible at large scale structure and the normalized energy density of the radiation $\Omega_r \approx 4.48 \times 10^{-5}$ [73]. In this situation, the numerical results of Eq. (89) are presented in Figs. 11 and 12 (see Appendix 11.1) for short- and long-wavelength modes respectively.

From all above plots, we see that the energy density fluctuations of a radiation fluid are growing-up in a very small scales with red-shift.

9 Matter density fluctuations in $f(T)$ gravity approach

Here, we consider the cosmic medium as a mixture of two non-interacting fluids as a torsion-dust and torsion-radiation mixture.

9.1 Torsion-dust system

In this fluid mixture, we assume that the Universe hosts two dominant cosmological fluids, namely a torsion-like fluid and the usual dust ($w_d = 0$) matter. In this case, evolution equation (66) reduces to

$$\ddot{\Delta}_d = \frac{\rho_d}{2f'} \Delta_d + \left(\frac{2f''}{3f'} \dot{T} - \theta \frac{2}{3} \right) \dot{\Delta}_d, \quad (91)$$

since $\Delta_m \approx \Delta_d$, $\rho_m = \rho_d$ and $\Omega_m = \Omega_d$. Then, we choose our paradigmatic $f(T)$ gravity model from Eq. (69) and applying Eq. (76) onto (91) yields

$$\ddot{\Delta}_d^k - (H\mathcal{Y} - 2H) \dot{\Delta}_d^k - \frac{3}{2} H^2 \Omega_d \Delta_d^k = 0. \quad (92)$$

We note that for the case of $n = 1$, the parameter $\mathcal{Y} = 0$ and Eq. (92) reduces to the well-known evolution equation of energy density of dust fluid in the GR limit namely

$$\ddot{\Delta}_d + 2H \dot{\Delta}_d - \frac{3}{2} H^2 \Omega_d \Delta_d^k = 0. \quad (93)$$

In red-shift space, it can be shown that Eq. (92) yields

$$\frac{d^2 \Delta_d^k}{dz^2} + \frac{1}{1+z} \left(\frac{4n-1}{3m} - 2 \right) \frac{d \Delta_d^k}{dz} - \frac{3 \Omega_d \Delta_d^k}{2(1+z)^2} = 0, \quad (94)$$

with the exact solution given as

$$\Delta_d^k(z) = C_1 (1+z)^{\frac{9m-4n+1+\varpi}{6m}} + C_2 (1+z)^{\frac{9m-4n+1-\varpi}{6m}}, \quad (95)$$

where

$$\varpi = \sqrt{(54\Omega_d + 81)m^2 - (72n - 18)m + (4n - 1)^2}. \quad (96)$$

Our free parameters Ω_d , m and n have a significant role to present the numerical solution of Eq. 95, and explore the growth of energy density fluctuations with red-shift.

⁶For Λ CDM limits $\Omega_r + \Omega_\Lambda = 1$ and for GR limit $\Omega_\Lambda = 0$, consequently, the solution of Eq. (85) and (88) have the same behavior.

Due to cosmic expansion, the background energy density of the dust fluid decreases with the scale factor of Universe, $\rho = \rho_0 a^{-3}$ and it is proportional to the red-shift z . Then, the scale factor becomes $a(t) = a_0(t/t_0)^{2/3(1+w_d)}$. To keep the generality of the ansatz in Eq. (70), we choose $m = 2/3(1+w_d) = 2/3$ for the scale factor exponent in Eq. (70) assuming a dust-dominated epoch. Consequently, Eq. (95) reads

$$\Delta_d^k(z) = C_1 (1+z)^{\frac{7-4n+\varpi}{4}} + C_2 (1+z)^{\frac{7-4n-\varpi}{4}}, \quad (97)$$

and in this suggestion, Eq. (96) reads

$$\varpi = \sqrt{16n^2 - 56n + 97 - 24/n}.$$

Here, ϖ has two complex and one real possible roots such as $r_{1,2} \approx 0.54522 \pm i0.57031$ and $n \approx 2.4096$. However, for illustrative purposes, we use different values of n for all numerical analysis and show that the $f(T)$ gravity model under consideration is an alternative approach to study the growth of the matter fluctuations in dust-dominated Universe and make a comparison with the well-known theory of gravity GR limit as well ⁷.

In order to fix the parameter Ω_d , we use either the definition of Eq.(78) for $n \geq 0.5$ or $\Omega_d = 0.32$ for any values of n . In the following, we apply these two options and explore the energy density contrast in $f(T)$ gravity approach systematically. For any case at $n = 1$, the numerical solution of $\delta(z)$ coincides with GR limit.

Case I: $\Omega_d = \frac{2n-1}{n}$, $n \geq 0.5$

To provide the parameter Ω_d , we use the definition from Eq.(78). From this definition, it is possible to determine the fractional amount of the normalized energy density parameters of the torsion (Ω_T) and dust (Ω_d) in the system. For instance, at $n = 1$, $\Omega_d = 1$ and Ω_T reads zero. In this case, the numerical solution is reduced to GR limit Eq. (83). For $n \geq 1$, $\Omega_d \geq 1$ and $\Omega_T \leq 0$, then, the dust fluid is the major component of the Universe and we note the contributions of torsion like fluid with negative energy density but $\rho = \rho_d + \rho_T \geq 0$. For $n = 0.9$, $\Omega_d \approx 0.88$ and $\Omega_T \approx 0.12$, meaning that the Universe has relatively more dust fluid than torsion fluid and at a particular $n \approx 0.5953$, the value of the normalized energy density parameter of dust fluid is favored with the observed value $\Omega_d \approx 0.32$ in SNIa data [72], consequently, $\Omega_T = 0.6800001$, and close to the observed value of $\Omega_\Lambda = 0.68$ [72]. With this values, we suggest that at $n \approx 0.595$, the growth of energy density fluctuations is occurred in the present torsion-dust era. For the case of $n = 0.5$, Ω_d reads zero and $\Omega_T = 1$. In this condition, the torsion fluid is large enough and the dust fluid is negligible in the torsion-dust system.

From the below Fig. 1 and Appendix 11.2 Figs. 13 and 14, we observe that the growth of the energy density fluctuations is nearly homogeneous initially, and growing-up with red-shift till near-future epoch for different values of $n \geq 0.5$.

For the case of $n = 1$ (red solid line) in Fig. 1, the growth of density fluctuations is the same as GR which is presented in Fig. 7. This once more indicates that our paradigmatic model is reduced to GR. Even if, at $n \approx 0.595$ (black solid line), the fluctuation of the energy density is growing-up with cosmic-time and similarly with the observed value of Ω_d presented in Fig. 8.

The growth of the fluctuations also is proportional to the values of n . For instance, at $n = 2$ (blue solid line) in Fig 13, the growth of energy density fluctuations is very high compared with other values of n presented in the plots.

Particularly, at $n = 0.5$, $\Omega_d = 0$ and $\Omega_T = 1$, with this, the numerical result of Eq. (95) is presented in Fig. 14 (blue solid line), and the growth of the fluctuations of dust fluid is nearly constant with red-shift.

Case II: $\Omega_d = 0.32$ and for any values of n

In this situation, we present the numerical result of Eq. (97) in Fig. 2 for different values of n . For $n = 1$ (red solid line) in Fig. 2 the density contrast has the same result as GR which is presented in Fig. 8. However, the growth the fluctuations is proportional to n values.

⁷N.B The first terms of the right-hand side of Eq. (97) is growing-up with red-shift so decaying with cosmic-time, and the second term is decaying with red-shift so growing with cosmic-time for any value of n .

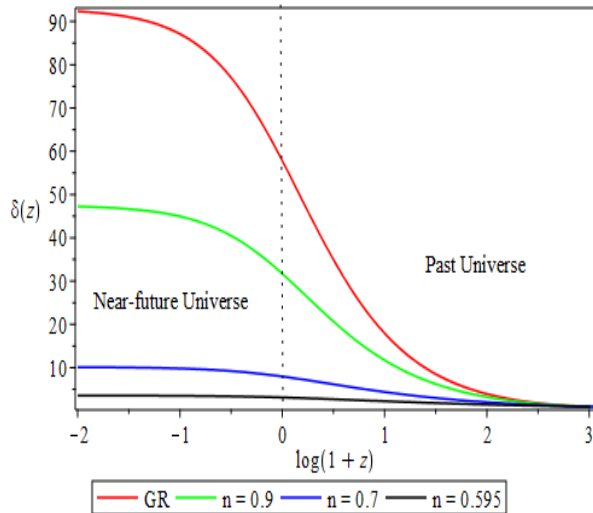


Figure 1: $\delta(z)$ versus z for Eq. (95) in the torsion-dust system for $n \leq 1$ and for $\Omega_d = \frac{2n-1}{n}$.

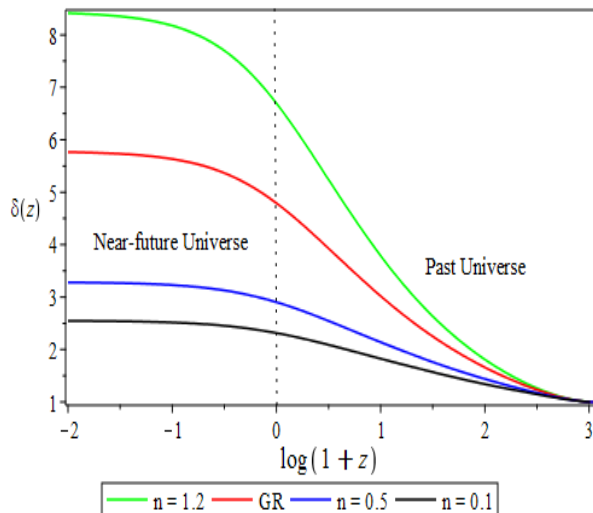


Figure 2: $\delta(z)$ versus z for Eq. (95) in the dust-torsion system for different value of n and for $\Omega_d = 0.32$.

We also study the matter density contrasts between $f(T)$ and GR approaches by using the definition in Eq. (80) and present the numerical results in Figs. 15 - 17 for both cases accordingly in the Appendix 11.2. In those figures, the comparison of dust perturbations between $f(T)$ gravity and GR is done by considering all above different values of n .

In general, we depict that our paradigmatic $f(T)$ gravity model is an alternative approach to study matter density contrast and the formation of large-scale. It explains the fluctuations of energy density in both cases and the fluctuations are growing-up for different intervals of n in the torsion-dust Universe. From all plots, we observe that our $f(T)$ gravity model has much gained an attention to explain the matter density contrast with range of $n \leq 1$ and favored with the usual results of GR. For instance, at $n = 1$, the result is exactly similar behavior with one of GR (dust-dominated universe), and for $n \approx 0.595$, it is favored with the observed value of $\Omega_d \approx 0.32$. However, the growth of the fluctuations is nearly constant with red-shift at $n = 0.5$ for the Case I alone. Whereas, at $n \gg 1$, the amplitude of the matter density contrast is very high and unrealistic to compare with the GR limit (see Fig. 13).

9.2 Torsion-radiation system

Here, we assume that the Universe is dominated by a torsion fluid and radiation ($w_r = 1/3$) mixture as a background, consequently the energy density of dust matter contribution is negligible. In such a system, perturbations would evolve according to the following equation (66)

$$\begin{aligned} \ddot{\Delta}_r^k = & \left[\frac{2}{3f'}\rho_r + \frac{1}{3f'}(f - Tf') - \frac{2f''}{9f'}\theta\dot{T} - \frac{k^2}{3a^2} + \right. \\ & \left. \left(\frac{2\rho_r f''}{f'^2} + \frac{2f''^2}{3f'^2}\theta\dot{T} - \frac{2f'''}{3f'}\theta\dot{T} \right) \frac{2\dot{T}\ddot{T}}{3\dot{T}^2} \right] \Delta_r^k + \left[\frac{f''}{3f'}\dot{T} \right. \\ & \left. + \frac{\theta}{3} + \left(\frac{2\rho_r f''}{f'^2} + \frac{2f''^2}{3f'^2}\theta\dot{T} - \frac{2f'''}{3f'}\theta\dot{T} \right) \frac{\dot{T}^2}{3\dot{T}^2} \right] \dot{\Delta}_r^k, \end{aligned} \quad (98)$$

i.e., $\Delta_m \approx \Delta_r$ and $\rho_m = \rho_r$. By applying our paradigmatic $f(T)$ gravity model and the power scale factor associated with Eqs. (76) and (77), it can be shown that the second-order evolution equation (98) of the energy density for torsion-radiation system can be re-written as

$$\begin{aligned} \ddot{\Delta}_r^k - H \left[\frac{\mathcal{Y}}{2} \left(1 + \frac{m}{3} \left(\Omega_r(1-n) - 2n + 3 \right) \right) - 1 \right] \dot{\Delta}_r^k \\ - H^2 \left[2n\Omega_r - 2\mathcal{X} - \mathcal{Y}(6-2n) - \frac{k^2}{3H^2 a^2} \right] \Delta_r^k = 0. \end{aligned} \quad (99)$$

For $n = 1$, this equation reduces to the well-known GR limit [32]:

$$\ddot{\Delta}_r^k + H\dot{\Delta}_r^k - \left(2H^2\Omega_r - \frac{k^2}{3a^2} \right) \Delta_r^k = 0. \quad (100)$$

Using Eqs. (71) - (74), we can re-write Eq. (99) in red-shift space as

$$\begin{aligned} \frac{d^2\Delta_r^k}{dz^2} + \frac{1}{1+z} \left[\frac{4(n-1)}{6m} \left(1 + \frac{m}{3} \left(\Omega_r(1-n) - 2n + 3 \right) \right) \right. \\ \left. + \frac{1}{m} - 1 \right] \frac{d\Delta_r^k}{dz} - \frac{1}{(1+z)^2} \left[2n\Omega_r - 2 \left(\frac{1-n}{n} \right) \right. \\ \left. + \frac{8}{3m} (n^2 - 4n + 3) - \frac{k^2}{3a^2 H^2} \right] \Delta_r^k(z) = 0. \end{aligned} \quad (101)$$

In the following two sub-sections, we further analyze the growth of energy density fluctuations from the solution of Eq. (101) in short- and long-wavelength modes.

9.2.1 Short-wavelength mode

Here, we discuss the growth of fractional energy density fluctuations within the horizon, where $k^2/a^2 H^2 \gg 1$. In this regime, the Jeans wavelength λ_J is much larger than the wavelength of the mean free path of the photon λ_p and the wavelength of the non-interacting fluid, i.e., $\lambda \ll \lambda_p \ll \lambda_J$ (see similar analysis: [37] for GR and [33] for $f(R)$ gravity theory approaches).

For further processing, we have to fix four basic parameters m , Ω_r , n and λ in Eq. (101) systematically. Here, we apply the same reason to fix the first parameter m as Sec. 9.1 for expanding Universe $\rho = \rho_0 a^{-4}$, and the scale factor becomes $a(t) = a_0(t/t_0)^{2/3(1+w_r)}$. Explicitly, we can choose our input parameter $m = 2/3(1+w) = 1/2$ for the scale factor exponent in Eq. (70) assuming we are in a radiation-dominated epoch. In this context our leading Eq. (101) reads

$$\begin{aligned} \frac{d^2\Delta_r^k}{dz^2} + \frac{1}{1+z} \left[\frac{4(n-1)}{3} \left(1 + \frac{1}{6} \left(\Omega_r(1-n) - 2n + 3 \right) \right) \right. \\ \left. + 1 \right] \frac{d\Delta_r^k}{dz} - \frac{1}{(1+z)^2} \left[2n\Omega_r - 2 \left(\frac{1-n}{n} \right) + \frac{16}{3} (n^2 - 4n + 3) \right. \\ \left. - \frac{16\pi^2}{3\lambda^2(1+z)^4} \right] \Delta_r^k(z) = 0. \end{aligned} \quad (102)$$

Let us define the following parameters as:

$$\begin{aligned}\beta &\equiv \frac{4(n-1)}{3} \left[1 + \frac{1}{6} (\Omega_r(1-n) - 2n + 3) \right] + 1, \\ \gamma &\equiv 2n\Omega_r - 2 \left(\frac{1-n}{n} \right) + \frac{16}{3} (n^2 - 4n + 3),\end{aligned}$$

then, our evolution equation Eq. (102) reads

$$\begin{aligned}\frac{d^2 \Delta_r^k}{dz^2} + \frac{\beta}{1+z} \frac{d\Delta_r^k}{dz} - \frac{1}{(1+z)^2} \left[\gamma \right. \\ \left. - \frac{16\pi^2}{3\lambda^2(1+z)^4} \right] \Delta_r^k(z) = 0.\end{aligned}\quad (103)$$

In the following, we consider three different cases to fix Ω_r and λ , and to see the effect of these parameters on the growth of fluctuations in the torsion-radiation system:

1. Using the definition of Ω_r presented in (78);
2. Using the observed value of Ω_r for different n ; and
3. Assuming $\gamma \ll \frac{16\pi^2}{3\lambda^2(1+z)^4}$ for small λ values.

In the following we consider the above three cases and discuss the growth of fluctuations in radiation-torsion system for short-wavelength range.

Case I: $\Omega_r = \frac{2n-1}{n}$, $n \geq 0.5$

In this case, we apply the definition of Ω_r presented in Eq. (78), and it is an essential point to know the amount of torsion and radiation fluids in the torsion-radiation system. In this situation, the above parameters β and γ read

$$\begin{aligned}\beta &\equiv \frac{4(n-1)}{3} \left[1 + \frac{1}{6} \left(\frac{(2n-1)(1-n)}{n} - 2n + 3 \right) \right] + 1, \\ \gamma &\equiv 2(2n-1) - 2 \left(\frac{1-n}{n} \right) + \frac{16}{3} (n^2 - 4n + 3),\end{aligned}$$

and the solution of the second-order evolution equation (103) admits

$$\begin{aligned}\Delta_r^k(z) &= C_1 (1+z)^{\frac{1}{2}(1-\beta)} \text{BesselJ} \left(\frac{\xi}{4}, \frac{2}{3} \frac{\sqrt{3}\pi}{\lambda(1+z)^2} \right) \\ &+ C_2 (1+z)^{\frac{1}{2}(1-\beta)} \text{BesselY} \left(\frac{\xi}{4}, \frac{2}{3} \frac{\sqrt{3}\pi}{\lambda(1+z)^2} \right),\end{aligned}\quad (104)$$

where

$$\xi = \sqrt{\beta^2 + 4\gamma - 2\beta + 1}.$$

For more clarity, the BesselJ and BesselY presented in Eq. (104) have increasing and decreasing behavior with red-shift respectively. For small values of n and λ , the second terms of the right hand-side Eq. (104) is decreasing with red-shift, in other words, increasing with cosmic-time and vis-versa for the first term of this equation. For $n = 1$, Eq. (103) is reduced to GR limit presented in Eq. (89).

Once we obtain the numerical solution (104), $\delta(z)$ and $\varrho(z)$ can easily be calculated by applying the definition of (79) and (80) respectively. By setting the parameter $m = 1/2$ and $\Omega_r = \frac{2n-1}{n}$, the parameter ξ reads

$$\begin{aligned}\xi &= \frac{\sqrt{2}}{9n} \left[32n^6 - 256n^5 + 1800n^4 - 4520n^3 \right. \\ &\left. + 3453n^2 - 430n + 2 \right]^{\frac{1}{2}},\end{aligned}\quad (105)$$

and it has four complex and two real possible roots such as $r_{1,2} \approx 2.3 \pm 5.7i$, $r_3 \approx 2.2$, $r_4 \approx 1.07$, $r_5 \approx 0.15$ and $r_6 \approx 0.005$.

Based on the definition of Ω_r , we consider $n \geq 0.5$ for numerical plotting and in these intervals of n , the value of ξ is always real. Apparently, at $n = 1$ the value of Ω_r becomes unity, Ω_T reads zero and $r = 2\sqrt{2}$, consequently, Eq. (104) reduces to radiation dominated case in GR limit.

For the case of $n \approx 0.5000112$, the value of $\Omega_r \approx 4.48 \times 10^{-5}$ and is closer to the observed value which presented in [73]. At $n = 0.5$, $\Omega_r = 0$ and $\Omega_T = 1$, the torsion fluid is the major component in torsion-radiation system.

For more clarity, we present the numerical results of the growth of energy density fluctuations for $n \gg 1$, $0.5 \leq n \leq 1$ and n is closer to one in the below Fig. 3 and Appendix 11.3.1 Figs. 19, 20.

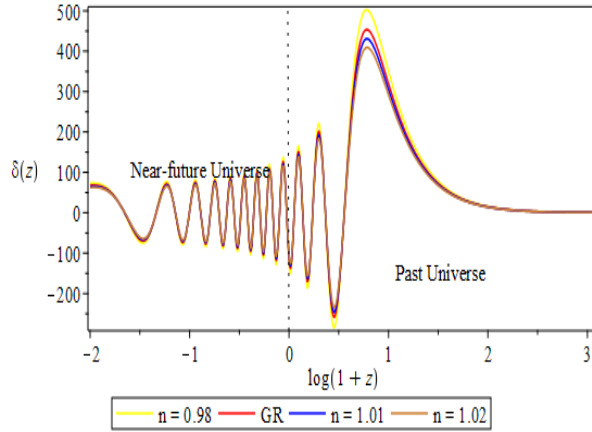


Figure 3: $\delta(z)$ versus z for Eq. (104) for n closer to GR limit and for $\Omega_r = \frac{2n-1}{n}$.

Case II: $\Omega_r \approx 4.48 \times 10^{-5}$ and for any values of n

Here, the detailed analysis of the growth of density fluctuations is done by taking the observed value of Ω_r and any values of n . By filling in for the value of Ω_r into Eq. (104), ξ reads

$$\xi \approx \sqrt{0.4n^4 - 2.2n^3 + 29n^2 - 95n + 76 - \frac{8}{n}}. \quad (106)$$

Then, ξ has two complex and three real roots such as $r_{1,2} \approx 0.90521 \pm 7.87304i$, $r_3 \approx 0.123664$, $r_4 \approx 2.56002$ and $r_5 \approx 1.0059$. In this situation, the values of ξ is changed by n dramatically. For example, from $0 < n \leq 0.123$, the value of ξ reads an imaginary value, and for $n > 0.123$, it reads real values, consequently, the numerical results of Eq. (104) is highly sensitive to the value of n . Explicitly, for $n = 1$, the numerical solution is exactly the same as the GR one presented in Fig. 11 and Fig. 4 (red solid line) for this case. For illustrative purposes, we shall assume $n \gg 1$, $n \ll 1$ and n is closer to GR in Fig. 4, and Fig. 21, 22 and 23 in the Appendix 11.3.1 accordingly.

Case III: For $\gamma \ll \frac{16\pi^2}{3\lambda^2(1+z)^4}$

For more simplicity, we assume a small value of λ and $\gamma \ll \frac{16\pi^2}{3\lambda^2(1+z)^4}$, the leading Eq. (103) reads

$$\frac{d^2 \Delta_r^k}{dz^2} + \frac{\beta}{1+z} \frac{d \Delta_r^k}{dz} + \frac{16\pi^2}{3\lambda^2(1+z)^6} \Delta_r^k(z) \approx 0, \quad (107)$$

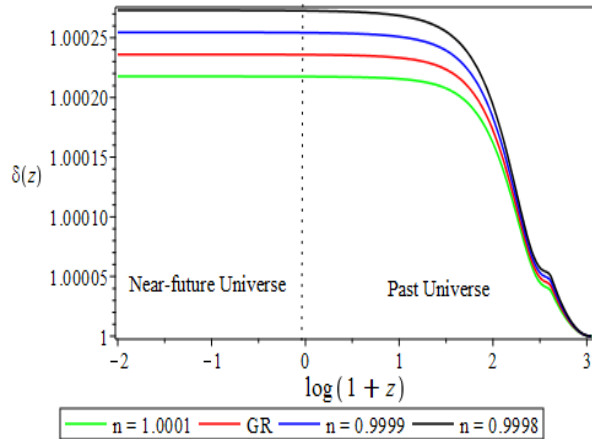


Figure 4: $\delta(z)$ versus z for Eq. (104) for n closed to GR limit and for $\Omega_r = 4.48 \times 10^{-5}$.

and the solution is

$$\begin{aligned} \Delta_r^k(z) = & C_1 (1+z)^{\frac{1}{2}(1-\beta)} \text{BesselJ} \left(\frac{\beta-1}{4}, \frac{2}{3} \frac{\sqrt{3}\pi}{\lambda (1+z)^2} \right) \\ & + C_2 (1+z)^{\frac{1}{2}(1-\beta)} \text{BesselY} \left(\frac{\beta-1}{4}, \frac{2}{3} \frac{\sqrt{3}\pi}{\lambda (1+z)^2} \right). \end{aligned} \quad (108)$$

In this limiting case, the parameter ξ becomes

$$\xi = \beta - 1 = \frac{4(n-1)}{3} \left[1 + \frac{1}{6} (\Omega_r(1-n) - 2n + 3) \right].$$

For the numerical results, we apply both cases I and II to fix Ω_r , and present the numerical results of Eq. (108) in Figs. 24 and 25 (see Appendix 11.3.1) for different values of n respectively. From these figures, we observe that the fluctuations grow in the past and decay in the present to near-future epoch.

In this sub-section, the energy density contrasts between $f(T)$ gravity and GR is done based on the definition of Eq. (80) in torsion-radiation system with short-wavelength mode and the numerical results is presented in Appendix 11.3.1 for Eq. (104) and (108) in Figs. 28 - 33 accordingly.

The detailed analysis of the growth of matter density fluctuations in torsion-radiation system for short-wavelength mode is made and it is convoluted for both cases and ranges of n , i.e., for $n \gg 1$, $n \ll 1$ and n closer to GR limits from Figs. 19 - 25 (see Appendix 11.3.1).

For instance, the growth of matter density contrasts in below Fig. 3 and Appendix 11.3.1 Figs. 20 and 22 have similar feature as GR and Λ CDM presented in Fig. 9. From these figures, we observe that the amplitude of the fluctuations $\delta(z)$ has oscillatory behavior, growing up in the past, decaying in the present epoch and becoming negligible in the near-future Universe. Moreover, the plots of energy density fluctuations in Fig. 4 (red solid line) has an exact behavior as the one in the GR limit in Fig. 11 for $n = 1$. From Figs. 24 and 25 (see Appendix 11.3.1), we observe that the growth of fluctuations is nearly constant initially, growing rapidly in the past and then start falling off in the present till near-future epoch and have similar growth features of $\delta(z)$ in the all ranges of n .

On the other hand, the amplitude of the oscillation of the matter density fluctuations presented in Figs. 19 and 21 (see Appendix 11.3.1) have extremely high and it is unrealistic to compare with the amplitude of matter fluctuations of the well-known results (GR and Λ CDM). Consequently, the amplitude of the corresponding matter density contrast between GR and $f(T)$ gravity in Figs. 26 and 29 (see Appendix 11.3.1) have the same feature. Eventually, for the case of $n \ll 1$ the growth of density perturbations in Fig. 23 (see Appendix 11.3.1) is unity at initial redshift and then decaying with red-shift till today which is totally ruled-out and unrealistic.

9.2.2 Long-wavelength mode

In the long-wavelength range where $k^2/a^2H^2 \ll 1$, all cosmological fluctuations begin and remain inside the Hubble horizon. With the k -dependences dropped, Eq. (103) admits an exact solution of the form

$$\Delta_r(z) = C_1 (1+z)^{\frac{1}{2}(1-\beta+\xi)} + C_2 (1+z)^{\frac{1}{2}(1-\beta-\xi)}. \quad (109)$$

For small values of n , the second term of the right hand-side of Eq. (109) is decaying with red-shift mean growing with cosmic-time and vis-versa for the first term of this equation. In the following, we also consider two cases for fixing the parameter Ω_r in long-wavelength range.

Case I: $\Omega_r = \frac{2n-1}{n}$, $n \geq 0.5$

We apply the definition of Eq. (78) and present the numerical plots of Eq. (109) for $n \gg 1$ and $0.5 \leq n \leq 1$ in below Fig. 5 and Appendix 11.3.2 in Fig. 35 accordingly for long-wavelength mode.

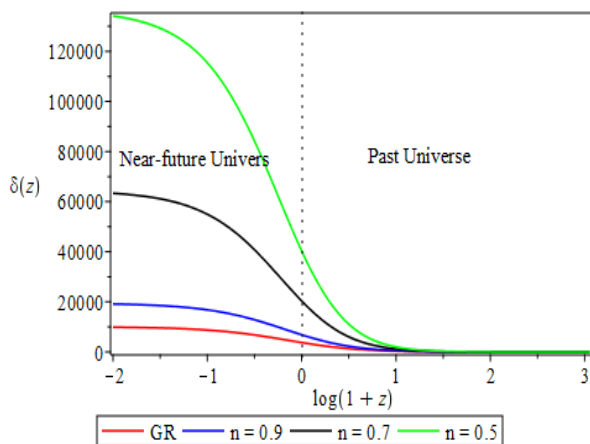


Figure 5: The growth of density fluctuations $\delta(z)$ versus z in long-wavelength mode for Eq. (109) for the values of $0.5 \leq n \leq 1$ and for $\Omega_d = \frac{2n-1}{n}$.

Case II: $\Omega_r = 4.48 \times 10^{-5}$ and for any values of n

Here we also present the numerical results of Eq. (109) in the blow Fig. 6 and Appendix 11.3.2 in Fig. 34 by taking $\Omega_r = 4.48 \times 10^{-5}$ for different values of n .

In the Figs. 35 - 36 (see in the Appendix 11.3.2), the energy density fluctuations of radiation fluid are growing with red-shift in long-wavelength mode but the amplitude of $\delta(z)$ is very high and unrealistic for the case of $n \gg 1$ to compare with either GR or Λ CDM results. Moreover, the result presented in Fig. 37 (see Appendix 11.3.2) is totally ruled-out and lost the reality of perturbations for the ranges of $n \ll 1$, because it is decaying with redshift. Fortunately, for n closer to GR limit, the growth of the fluctuations has similar behavior as the GR, see Figs. 5 and 6 with Figs. 10 and 12 in the Appendix 11.3.2 for detail. We also present the matter density contrast between $f(T)$ and GR for long-wavelength mode in the Appendix 11.3.2 for all cases accordingly.

In general, $f(T)$ gravity theory has gained much attention for different cosmological implications and it is shown that the $f(T)$ gravity can be an alternative approach to study the growth of energy density fluctuations for torsion-dust and torsion-radiation systems with $1+3$ covariant formalism by applying the paradigmatic $f(T)$ gravity model in Eq. (69) with power scale factor. We presented the numerical results of Eq. (66), for analyzing the growth of energy density fluctuations from past to near-future in both systems.

Unquestionably, our paradigmatic $f(T)$ gravity model is an alternative approach to explain cosmological perturbations and formation of large-scale structures for n closer to GR limit. However, it is not favored for $n \ll 1$ (see Figs 23 and 37) (see Appendix 11.3.1 and 11.3.2 respectively), in these intervals of n , the value

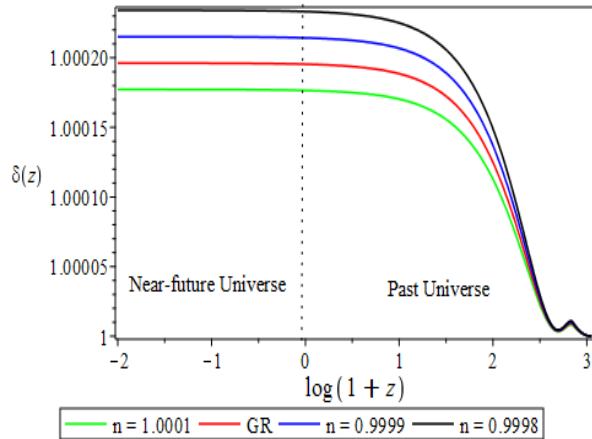


Figure 6: The growth of density fluctuations $\delta(z)$ versus z in long-wavelength mode for Eq. (109) for the values of n closer to GR and for $\Omega_r = 4.48 \times 10^{-5}$.

of ξ reads an imaginary value and the corresponding numerical plots are totally contradicting the well-known results of GR and Λ CDM limits. From all cases, the corresponding numerical results of density fluctuations are nearly constant at large red-shift, growing up in the past, decaying in the present and become negligible in the near-future possibly cosmic expansion in torsion-radiation system.

10 Conclusions

This paper presented a detailed analysis of scalar cosmological perturbations in $f(T)$ gravity theory using the $1+3$ covariant gauge-invariant formalism. We defined the gauge-invariant variables and derived the corresponding evolution equations. Then, the harmonic decomposition technique was applied to make the equations manageable for analysis. From that, we obtained exact solutions of the evolution equations for both torsion-radiation and torsion-dust two-fluid systems after considering the quasi-static approximation, and computed the growth of the fractional energy density perturbations $\delta(z)$ and the deviation from GR values, $\varrho(z)$, for the well-known power-law $f(T)$ gravity model and the power-law cosmological scale factor. For the torsion-dust system, we studied the behavior of dust perturbations and observed that $\delta(z)$ is growing with cosmic time. In the torsion-radiation system, we considered short-wavelength and long-wavelength modes. It is observed that the growth of matter density fluctuations for both modes and the matter density contrast change dramatically for different ranges of n considered, i.e., for $n \gg 1$, $n \ll 1$ and n closer to GR limits. The matter density contrasts in our paradigmatic $f(T)$ gravity model are consistent with GR predictions for n closer to one, these models are not favored in the range $n \ll 1$ as the linearity of the perturbations is broken. It is evident from our preliminary results that our $f(T)$ model results contain a richer set of possibilities whose model parameters can be constrained using up-and-coming observational data and can accommodate currently known features of the large-scale structure power spectrum in the general relativistic and Λ CDM limits. We envisage to undertake this aspect of the task for more realistic $f(T)$ models in a multi-fluid cosmological fluid setting in a subsequent work.

Acknowledgements

SS gratefully acknowledges financial support from Wolkite University and Entoto Observatory and Research Center, Ethiopian Space Science and Technology Institute. JN gratefully acknowledges financial support from the Swedish International Development Cooperation Agency (SIDA) through the International Science Program (ISP) to the University of Rwanda (Rwanda Astrophysics, Space and Climate Science Research Group), project number RWA01. DFM thanks the Research Council of Norway for their support. The simulations were performed on resources provided by UNINETT Sigma2, the National Infrastructure for High Performance Computing and Data Storage in Norway. This paper is based upon work from the COST action CA15117 (CANTATA), supported by COST (European Cooperation in Science and Technology). AA acknowledges that this work is based on the research supported in part by the National Research Foundation (NRF) of South Africa

with grant numbers 109257 and 112131. AdlCD acknowledges financial support from Project No. FPA2014-53375-C2-1-P from the Spanish Ministry of Economy and Science, Project No. FIS2016-78859-P from the European Regional Development Fund and Spanish Research Agency (AEI), Project No. CA16104 from COST Action EU Framework Programme Horizon 2020, University of Cape Town Launching Grants Programme and National Research Foundation Grants No. 99077 2016-2018, Ref. No. CSUR150628121624, 110966 Ref. No. BS170509230233, and the NRF Incentive Funding for Rated Researchers (IPRR), Ref. No. IFR170131220846. SS, JN and AA are grateful for the Institute of Theoretical Astrophysics, University of Oslo, for hosting them during the initial preparation of this manuscript.

References

- [1] A. G. Riess *et al.*, “Observational evidence from supernovae for an accelerating universe and a cosmological constant,” *The Astronomical Journal*, vol. 116, no. 3, p. 1009, 1998.
- [2] S. Perlmutter *et al.*, “Discovery of a supernova explosion at half the age of the universe,” *Nature*, vol. 391, no. 6662, pp. 51–54, 1998.
- [3] A. H. Guth, “Inflationary universe: A possible solution to the horizon and flatness problems,” *Physical Review D*, vol. 23, no. 2, p. 347, 1981.
- [4] A. R. Liddle, D. H. Lyth, and R. A. Daly, “Cosmological inflation and large-scale structure,” *Physics Today*, vol. 54, no. 7, p. 56, 2001.
- [5] A. Guth, “Inflation and cosmological perturbations,” *The Future of Theoretical Physics and Cosmology*, pp. 725–754, 2003.
- [6] E. Kolb, *The early universe*. CRC Press, 2018.
- [7] M. Longair and R. Sunyaev, “Fluctuations in the microwave background radiation,” *Nature*, vol. 223, no. 5207, pp. 719–721, 1969.
- [8] R. Sunyaev, “Fluctuations of the microwave background radiation,” in *Symposium-International Astronomical Union*, vol. 79, pp. 393–404, Cambridge University Press, 1978.
- [9] A. Miller *et al.*, “A measurement of the angular power spectrum of the cosmic microwave background from $l = 100$ to 400,” *The Astrophysical Journal Letters*, vol. 524, no. 1, p. L1, 1999.
- [10] S. Hawking, “Perturbations of an expanding universe,” *The Astrophysical Journal*, vol. 145, p. 544, 1966.
- [11] E. R. Harrison, “Fluctuations at the threshold of classical cosmology,” *Physical Review D*, vol. 1, no. 10, p. 2726, 1970.
- [12] J. M. Bardeen, “Gauge-invariant cosmological perturbations,” *Physical Review D*, vol. 22, no. 8, p. 1882, 1980.
- [13] K. S. Thorne, “Multipole expansions of gravitational radiation,” *Reviews of Modern Physics*, vol. 52, no. 2, p. 299, 1980.
- [14] V. F. Mukhanov, “Quantum theory of gauge-invariant cosmological perturbations,” *Zh. Eksp. Teor. Fiz.*, vol. 94, no. 1, 1988.
- [15] P. J. Peebles and J. Yu, “Primeval adiabatic perturbation in an expanding universe,” *The Astrophysical Journal*, vol. 162, p. 815, 1970.
- [16] L. Searle and R. Zinn, “Compositions of halo clusters and the formation of the galactic halo,” *The Astrophysical Journal*, vol. 225, pp. 357–379, 1978.
- [17] K. Freeman and J. Bland-Hawthorn, “The new galaxy: signatures of its formation,” *Annual Review of Astronomy and Astrophysics*, vol. 40, no. 1, pp. 487–537, 2002.
- [18] J. S. Bullock and K. V. Johnston, “Tracing galaxy formation with stellar halos. I. Methods,” *The Astrophysical Journal*, vol. 635, no. 2, p. 931, 2005.

- [19] G. R. Blumenthal, S. Faber, J. R. Primack, and M. J. Rees, “Formation of galaxies and large-scale structure with cold dark matter,” *Nature*, vol. 311, no. 5986, p. 517, 1984.
- [20] D. Liu and M. Reboucas, “Energy conditions bounds on $f(T)$ gravity,” *Physical Review D*, vol. 86, no. 8, p. 083515, 2012.
- [21] C. Li, Y. Cai, Y.-F. Cai, and E. N. Saridakis, “The effective field theory approach of teleparallel gravity, $f(T)$ gravity and beyond,” *arXiv preprint arXiv:1803.09818*, 2018.
- [22] Y.-F. Cai, Capozziello, M. De Laurentis, and E. N. Saridakis, “ $f(T)$ teleparallel gravity and cosmology,” *arXiv preprint arXiv:1511.07586*, 2015.
- [23] Á. De la Cruz-Dombriz, P. K. Dunsby, and D. Sáez-Gómez, “Junction conditions in extended teleparallel gravities,” *Journal of Cosmology and Astroparticle Physics*, vol. 2014, no. 12, p. 048, 2014.
- [24] A. Paliathanasis, J. L. Said, and J. D. Barrow, “Stability of the Kasner Universe in $f(T)$ Gravity,” tech. rep., 2017.
- [25] S. Capozziello, G. Lambiase, and C. Stornaiolo, “Geometric classification of the torsion tensor in space-time,” *arXiv preprint gr-qc/0101038*, 2001.
- [26] S. Kar and S. Sengupta, “The Raychaudhuri equations: A brief review,” *Pramana*, vol. 69, no. 1, pp. 49–76, 2007.
- [27] K. Pasmatsiou, C. G. Tsagas, and J. D. Barrow, “Kinematics of einstein-cartan universes,” *Physical Review D*, vol. 95, no. 10, p. 104007, 2017.
- [28] S. Sahlu, J. Ntahompagaze, M. Elmardi, and A. Abebe, “The Chaplygin Gas as a Model for $f(T)$ Gravitation?,” *arXiv preprint arXiv:1904.09897*, 2019.
- [29] R. C. Nunes, “Structure formation in $f(T)$ gravity and a solution for h_0 tension,” *Journal of Cosmology and Astroparticle Physics*, vol. 2018, no. 05, p. 052, 2018.
- [30] H. Kodama and M. Sasaki, “Cosmological perturbation theory,” *Progress of Theoretical Physics Supplement*, vol. 78, pp. 1–166, 1984.
- [31] E. M. Lifshitz, “On the gravitational stability of the expanding universe,” *Zhurnal Eksperimentalnoi i Teoreticheskoi Fiziki*, vol. 16, pp. 587–602, 1946.
- [32] S. Carloni, “Covariant Gauge Invariant Theory of Scalar Perturbations in $f(R)$ -Gravity: A Brief Review,” *Open Astronomy Journal*, vol. 3, pp. 76–93, 2010.
- [33] A. Abebe, M. Abdelwahab, Á. De la Cruz-Dombriz, and P. K. Dunsby, “Covariant gauge-invariant perturbations in multifluid $f(R)$ gravity,” *Class. Quant. Grav.*, vol. 29, no. 13, p. 135011, 2012.
- [34] G. Ellis, “InProceedings of the International School of Physics Enrico Fermi, XLVII: General Relativity and Cosmology, 1969,” 1971.
- [35] G. F. Ellis and M. Bruni, “Covariant and gauge-invariant approach to cosmological density fluctuations,” *Physical Review D*, vol. 40, no. 6, p. 1804, 1989.
- [36] J. M. Stewart and M. Walker, “Perturbations of space-times in general relativity,” in *Proceedings of the Royal Society of London A: Mathematical, Physical and Engineering Sciences*, vol. 341, pp. 49–74, The Royal Society, 1974.
- [37] P. K. Dunsby, “Gauge invariant perturbations in multi-component fluid cosmologies,” *Class. Quant. Grav.*, vol. 8, no. 10, p. 1785, 1991.
- [38] P. K. Dunsby, M. Bruni, and G. F. Ellis, “Covariant perturbations in a multifluid cosmological medium,” *The Astrophysical Journal*, vol. 395, pp. 54–74, 1992.
- [39] M. Bruni, P. K. Dunsby, and G. F. Ellis, “Cosmological perturbations and the physical meaning of gauge-invariant variables,” *The Astrophysical Journal*, vol. 395, pp. 34–53, 1992.

- [40] J. Ntahompagaze, A. Abebe, and M. Mbonye, “A study of perturbations in scalar–tensor theory using 1+3 covariant approach,” *Int. J. Mod. Phys. D*, vol. 27, no. 3, p. 1850033, 2018.
- [41] B. Li, T. P. Sotiriou, and J. D. Barrow, “Large-scale structure in $f(T)$ gravity,” *Physical Review D*, vol. 83, no. 10, p. 104017, 2011.
- [42] K. Hayashi and T. Nakano, “Extended translation invariance and associated gauge fields,” *Progress of Theoretical Physics*, vol. 38, no. 2, pp. 491–507, 1967.
- [43] G. R. Bengochea and R. Ferraro, “Dark torsion as the cosmic speed-up,” *Physical Review D*, vol. 79, no. 12, p. 124019, 2009.
- [44] E. V. Linder, “Einstein’s other gravity and the acceleration of the universe,” *Physical Review D*, vol. 81, no. 12, p. 127301, 2010.
- [45] S. Basilakos, “Linear growth in power law $f(T)$ gravity,” *Physical Review D*, vol. 93, no. 8, p. 083007, 2016.
- [46] M. Setare and F. Darabi, “Power-law solutions in $f(T)$ gravity,” *General Relativity and Gravitation*, vol. 44, no. 10, pp. 2521–2527, 2012.
- [47] J. Noller, F. von Braun-Bates, and P. G. Ferreira, “Relativistic scalar fields and the quasistatic approximation in theories of modified gravity,” *Physical Review D*, vol. 89, no. 2, p. 023521, 2014.
- [48] S. Peirone, K. Koyama, L. Pogosian, M. Raveri, and A. Silvestri, “Large-scale structure phenomenology of viable horndeski theories,” *Physical Review D*, vol. 97, no. 4, p. 043519, 2018.
- [49] S. Bose, “Testing the quasi-static approximation in $f(R)$ gravity simulations,” in *Beyond Λ CDM*, pp. 103–138, Springer, 2018.
- [50] G. F. Ellis, “Relativistic cosmology,” *Cargese lectures in Physics*, vol. 6, pp. 1–60, 1973.
- [51] J. M. Stewart and M. Walker, “Perturbations of space-times in general relativity,” in *Proceedings of the Royal Society of London A: Mathematical, Physical and Engineering Sciences*, vol. 341, pp. 49–74, The Royal Society, 1974.
- [52] G. F. Ellis and H. Van Elst, “Cosmological models,” in *Theoretical and Observational Cosmology*, pp. 1–116, Springer, 1999.
- [53] F. Darabi, M. Mousavi, and K. Atazadeh, “Geodesic deviation equation in $f(T)$ gravity,” *Physical Review D*, vol. 91, no. 8, p. 084023, 2015.
- [54] B. Li, T. P. Sotiriou, and J. D. Barrow, “ $f(T)$ gravity and local lorentz invariance,” *Physical Review D*, vol. 83, no. 6, p. 064035, 2011.
- [55] G. F. Ellis, R. Maartens, and M. A. MacCallum, *Relativistic cosmology*. Cambridge University Press, 2012.
- [56] P. KS Dunsby *et al.*, “Cosmological perturbations and the physical meaning of gauge-invariant variables,” *Astrophysical Journal*, vol. 395, p. 34, 1992.
- [57] S. W. Hawking and G. F. R. Ellis, *The large scale structure of space-time*, vol. 1. Cambridge University Press, 1973.
- [58] G. F. Ellis and H. Van Elst, “Cosmological models,” in *Theoretical and Observational Cosmology*, pp. 1–116, Springer, 1999.
- [59] C. Castaneda *et al.*, *Some Aspects in Cosmological Perturbation Theory and $f(R)$ Gravity*. PhD thesis, Dissertation, Bonn, Rheinische Friedrich-Wilhelms-Universität Bonn, 2016, 2016.
- [60] J. Ehlers, “AK Raychaudhuri and his equation,” *Pramana*, vol. 69, no. 1, pp. 7–14, 2007.
- [61] S. Carloni, P. K. Dunsby, and C. Rubano, “Gauge invariant perturbations of scalar-tensor cosmologies: The vacuum case,” *Physical Review D*, vol. 74, no. 12, p. 123513, 2006.
- [62] K. N. Ananda, S. Carloni, and P. K. Dunsby, “A detailed analysis of structure growth in $f(R)$ theories of gravity,” *Class. Quant. Grav.*, vol. 26, no. arXiv: 0809.3673, p. 235018, 2008.

- [63] G. Ballesteros and J. Lesgourgues, “Dark energy with non-adiabatic sound speed: initial conditions and detectability,” *Journal of Cosmology and Astroparticle Physics*, vol. 2010, no. 10, p. 014, 2010.
- [64] S. Carloni, P. Dunsby, and A. Troisi, “Evolution of density perturbations in $f(R)$ gravity,” *Physical Review D*, vol. 77, no. 2, p. 024024, 2008.
- [65] A. Abebe, “Breaking the cosmological background degeneracy by two-fluid perturbations in $f(R)$ gravity,” *Int. J. Mod. Phys. D*, vol. 24, no. 07, p. 1550053, 2015.
- [66] S. Nojiri and S. D. Odintsov, “Introduction to modified gravity and gravitational alternative for dark energy,” *Int. J. Geom. Methods Mod. Phys.*, vol. 4, no. 01, pp. 115–145, 2007.
- [67] S. Bahamonde, S. Odintsov, V. Oikonomou, and M. Wright, “Correspondence of $F(R)$ gravity singularities in Jordan and Einstein frames,” *Annals of Physics*, vol. 373, pp. 96–114, 2016.
- [68] G. F. Smoot *et al.*, “Structure in the coBE differential microwave radiometer first-year maps,” *The Astrophysical Journal*, vol. 396, pp. L1–L5, 1992.
- [69] R. Sachs and A. Wolfe, “Perturbations of a cosmological model and angular variations of the microwave background,” 1967.
- [70] W. Hu, “CMB temperature and polarization anisotropy fundamentals,” *arXiv preprint astro-ph/0210696*, 2002.
- [71] A. Abebe, Á. de la Cruz-Dombriz, and P. K. Dunsby, “Large scale structure constraints for a class of $f(R)$ theories of gravity,” *Physical Review D*, vol. 88, no. 4, p. 044050, 2013.
- [72] P. A. Ade *et al.*, “Planck 2015 results: XIII. Cosmological parameters,” 2016.
- [73] P.-H. Chavanis, “Cosmology with a stiff matter era,” *Physical Review D*, vol. 92, no. 10, p. 103004, 2015.

11 Appendix: The energy density contrasts

11.1 For GR Λ CDM approaches

In the following figures, we present the energy density contrasts in GR and Λ CDM approaches.

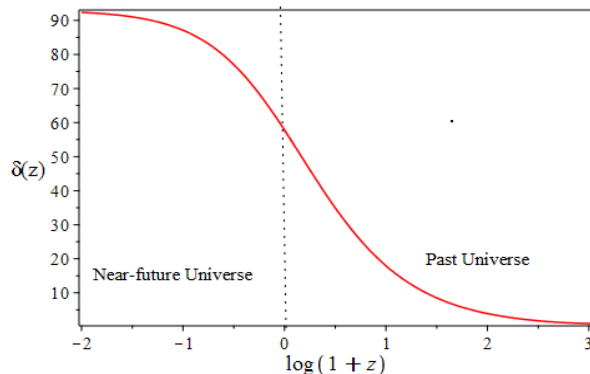


Figure 7: The density contrasts $\delta(z)$ versus red-shift z for Eq. (84) for dust-dominated Universe. We use $\Omega_d = 1$ for illustrative purpose.

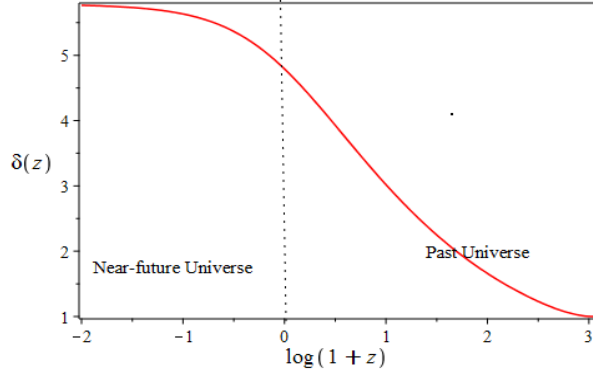


Figure 8: The illustrative of density contrasts $\delta(z)$ with z for Eq. (84) for dust Universe and for $\Omega_d = 0.32$.

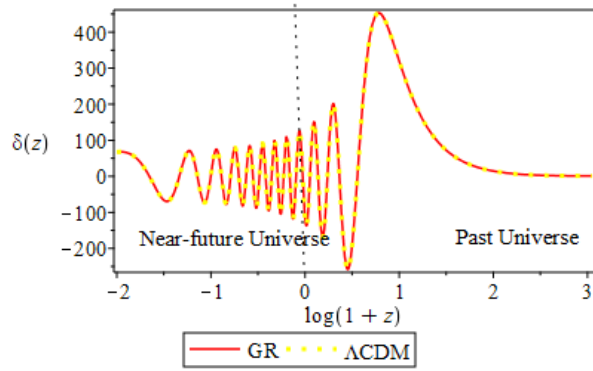


Figure 9: $\delta(z)$ versus z for Eqs. (86) (yellow dotted line) and (89) (red solid line) for short-wavelength mode in the radiation-dominated Universe. We consider $\Omega_r = 1 - \Omega_\Lambda$ and $\lambda = 0.05\text{Mpc}$ for plotting.

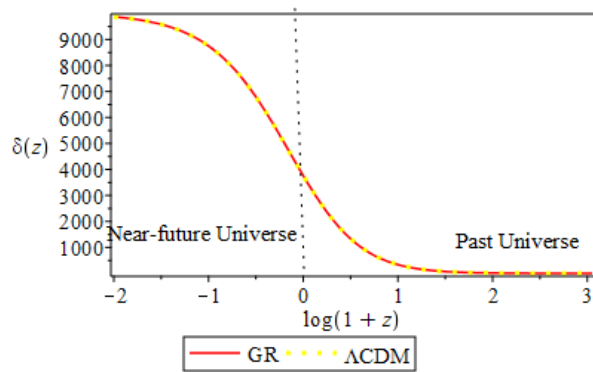


Figure 10: $\delta(z)$ versus z for Eqs. (86) (yellow dotted line) and (89) (red solid line) for long-wavelength mode in radiation-dominated Universe and for $\Omega_r = 1 - \Omega_\Lambda$.

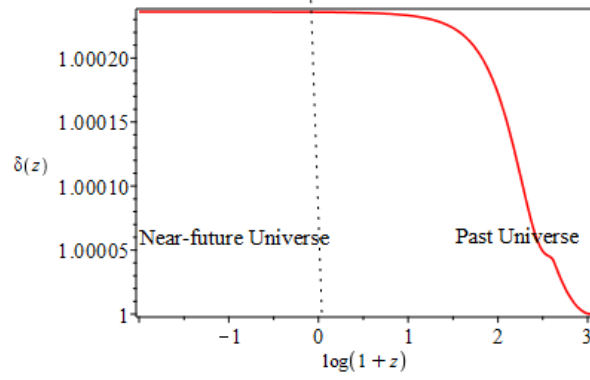


Figure 11: The numerical results of $\delta(z)$ versus z for Eq. (89) for short-wavelength mode mode. We use the prospective value of $\Omega_r = 4.48 \times 10^{-5}$ for plotting.

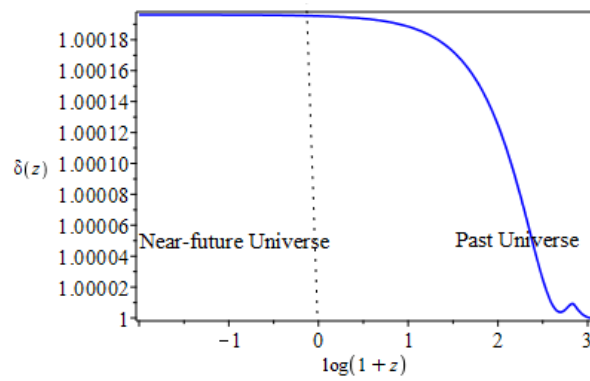


Figure 12: The numerical results of $\delta(z)$ versus z for Eq. (89) for long-wavelength mode mode and for $\Omega_r = 4.48 \times 10^{-5}$ for plotting.

11.2 Dust-torsion system

Here, we also present the energy density contrasts in $f(T)$ gravity approach. The energy density contrast

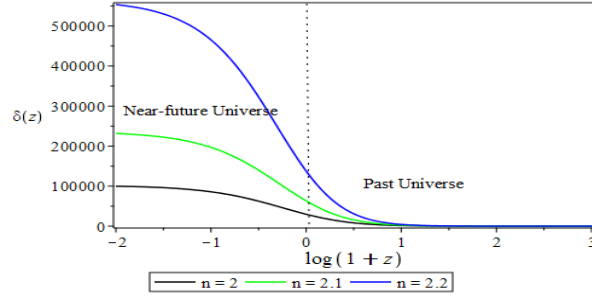


Figure 13: $\delta(z)$ versus z for Eq. (95) in the torsion-dust system for $n \gg 1$ and for $\Omega_d = \frac{2n-1}{n}$.

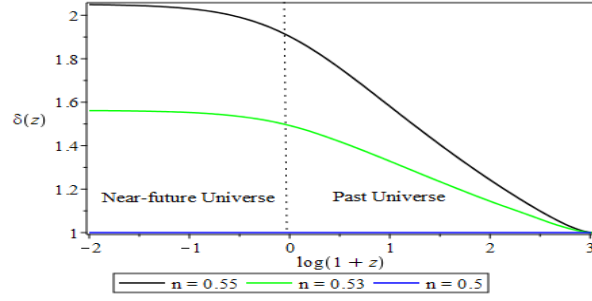


Figure 14: $\delta(z)$ versus z for Eq. (95) in the dust-torsion system for the values of $0.5 \leq n < 0.595$ and for $\Omega_d = \frac{2n-1}{n}$.

between $f(T)$ and GR approaches by applying definition Eq. (80) for torsion-dust system in Figs. 15 - 18. As we mentioned, the density contrast $\varrho(z)$ is zero for the case of $n = 1$.

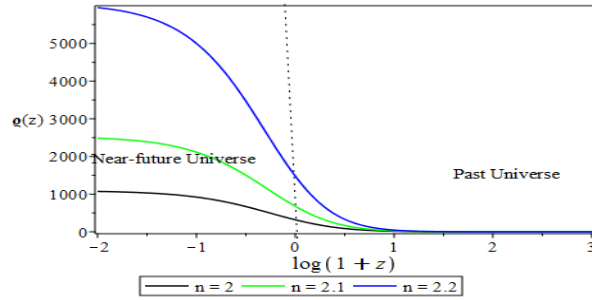


Figure 15: $\varrho(z)$ versus z for Eq. (95) in the torsion-dust system for $n \gg 1$ and for $\Omega_d = \frac{2n-1}{n}$.

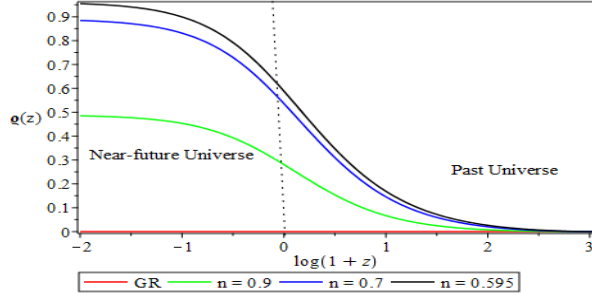


Figure 16: $\rho(z)$ versus z for Eq. (95) in the torsion-dust system for $n \leq 1$ and for $\Omega_d = \frac{2n-1}{n}$.

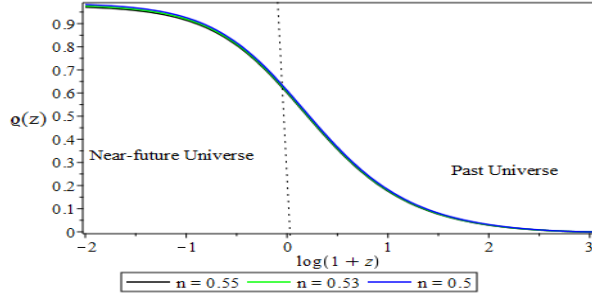


Figure 17: $\rho(z)$ versus z for Eq. (95) in the dust-torsion system for the values of $0.5 \leq n < 0.595$ and for $\Omega_d = \frac{2n-1}{n}$.

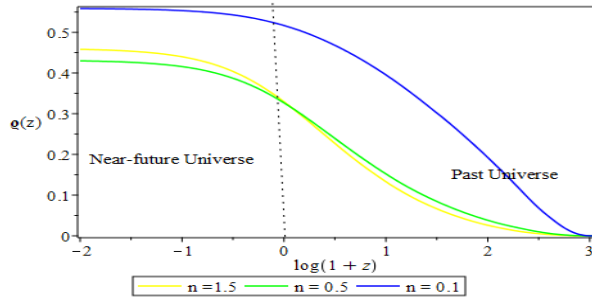


Figure 18: $\rho(z)$ versus z for Eq. (95) in the dust-torsion system for different value of n and for $\Omega_d = 0.32$.

11.3 Torsion-radiation System

11.3.1 Short-wavelength

In the following, the matter density contrasts is presented in torsion-radiation system for short-wavelength range for different range of n and for different cases.

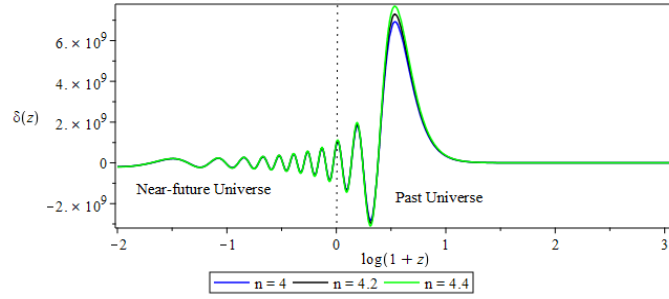


Figure 19: $\delta(z)$ versus z for Eq. (104) for $n \gg 1$ and for $\Omega_r = \frac{2n-1}{n}$.

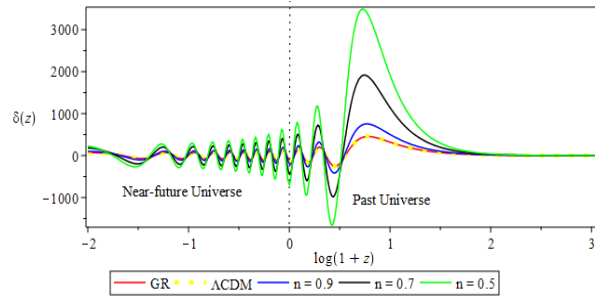


Figure 20: $\delta(z)$ versus z for Eq. (104) for $0.5 \leq n \leq 1$ and for $\Omega_r = \frac{2n-1}{n}$.

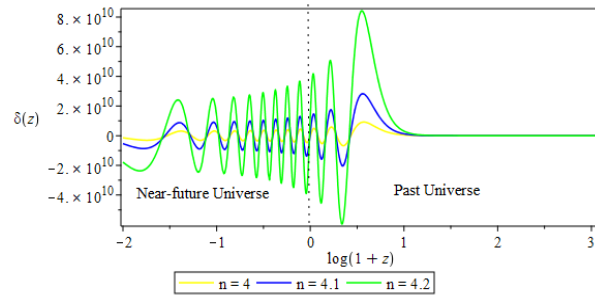


Figure 21: $\delta(z)$ versus z for Eq. (104) for $n \gg 1$ and for $\Omega_r = 4.48 \times 10^{-5}$.

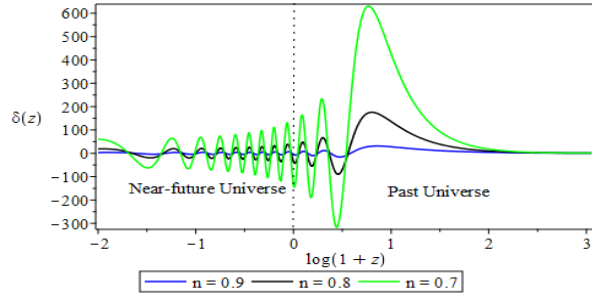


Figure 22: $\delta(z)$ versus z for Eq. (104) for $n < 1$ and for $\Omega_r = 4.48 \times 10^{-5}$.

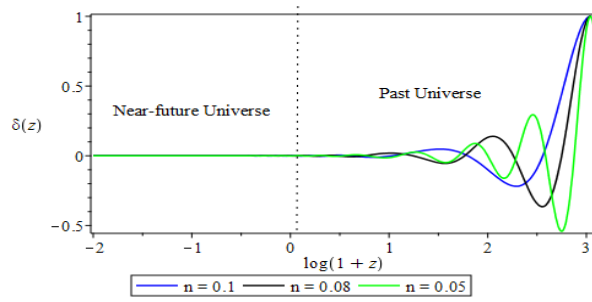


Figure 23: $\delta(z)$ versus z for Eq. (104) for $n \ll 1$ and for $\Omega_r = 4.48 \times 10^{-5}$.

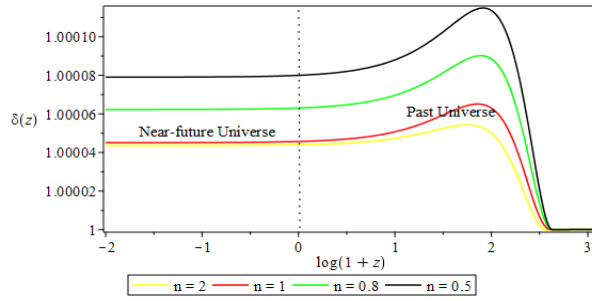


Figure 24: $\delta(z)$ versus z for Eq. (108) and for different values of n and for $\Omega_r = \frac{2n-1}{n}$.

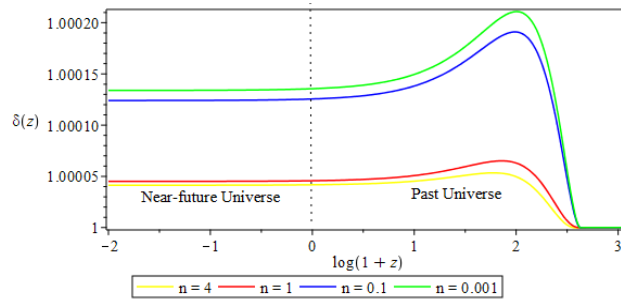


Figure 25: $\delta(z)$ versus z for Eq. (108) in the short-wavelength mode for different values of n and for $\Omega_r = 4.48 \times 10^{-5}$.

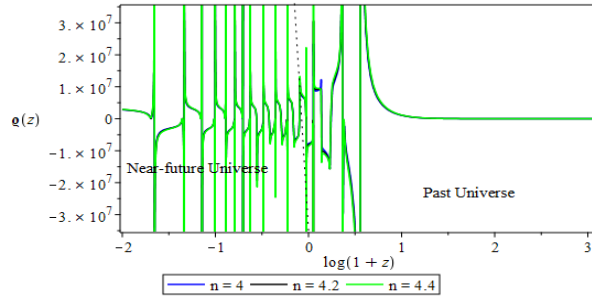


Figure 26: $\varrho(z)$ versus z for Eq. (108) and for $n \gg 1$.

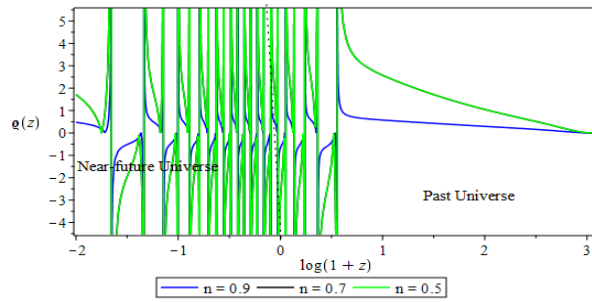


Figure 27: $\varrho(z)$ versus z for Eq. (104) in the short-wavelength mode for $0.5 \leq n \leq 1$.

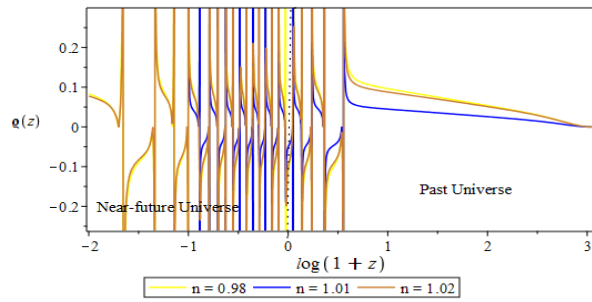


Figure 28: $\varrho(z)$ versus z for Eq. (108) and for $n \gg 1$.

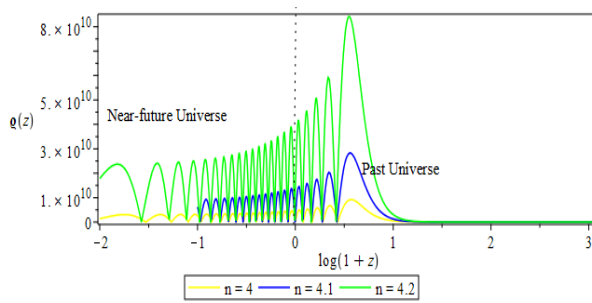


Figure 29: $\varrho(z)$ versus z for Eq. (104) in the short-wavelength mode for $0.5 \leq n \leq 1$.

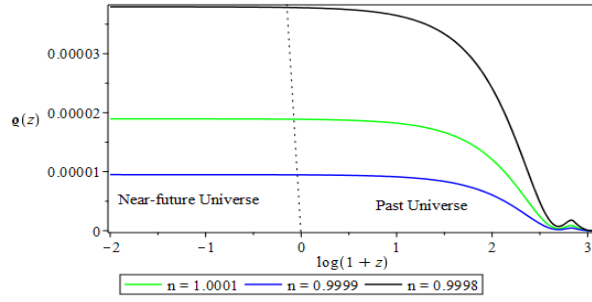


Figure 30: $\varrho(z)$ versus z for Eq. (104) for n closed to GR limit and for $\Omega_r = 4.48 \times 10^{-5}$.

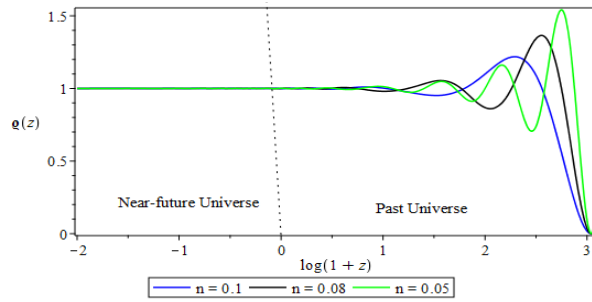


Figure 31: $\varrho(z)$ versus z for Eq. (104) for $n \ll 1$ and for $\Omega_r = 4.48 \times 10^{-5}$.

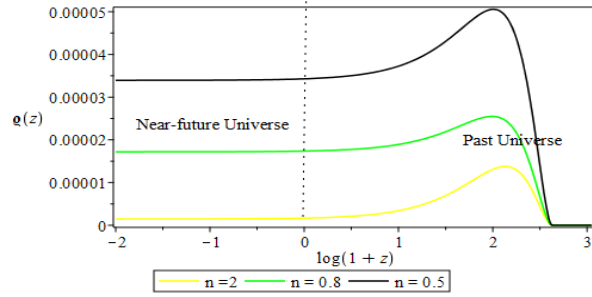


Figure 32: $\varrho(z)$ versus z for Eq. (108) in the short-wavelength mode for $0.5 \leq n \leq 1$.

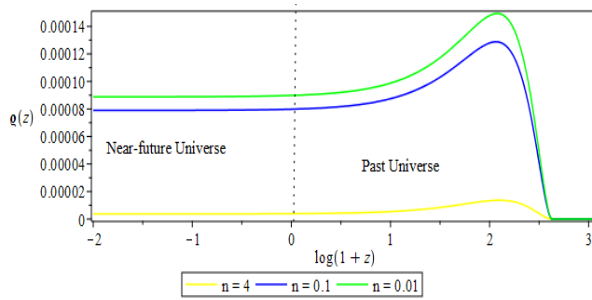


Figure 33: $\varrho(z)$ versus z for Eq. (104) for $n \gg 1$ and for $\Omega_r = 4.48 \times 10^{-5}$.

11.3.2 Long-wavelength

The matter density contrasts is presented in torsion-radiation system for long-wavelength for different cases.

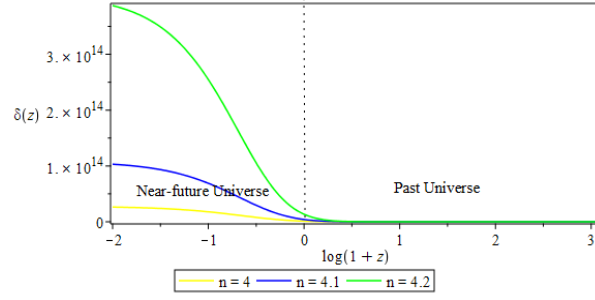


Figure 34: The growth of density fluctuations $\delta(z)$ versus z in long-wavelength mode for Eq. (109) for the values of $n \gg 1$ and for $\Omega_r = 4.48 \times 10^{-5}$.

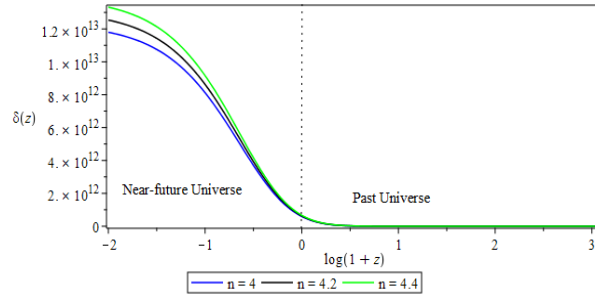


Figure 35: The growth of density fluctuations $\delta(z)$ versus z in long-wavelength mode for Eq. (109) for the values of $n \gg 1$ and for $\Omega_r = \frac{2n-1}{n}$.

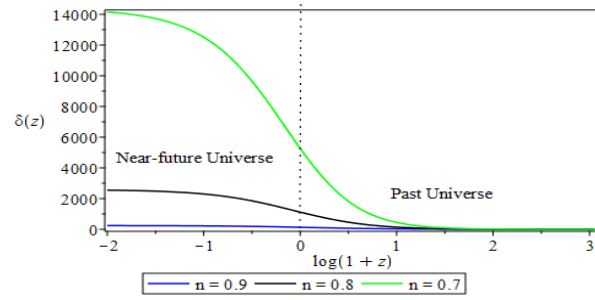


Figure 36: The growth of density fluctuations $\delta(z)$ versus z in long-wavelength mode for Eq. (109) for the values of $n < 1$ and for $\Omega_r = 4.48 \times 10^{-5}$.

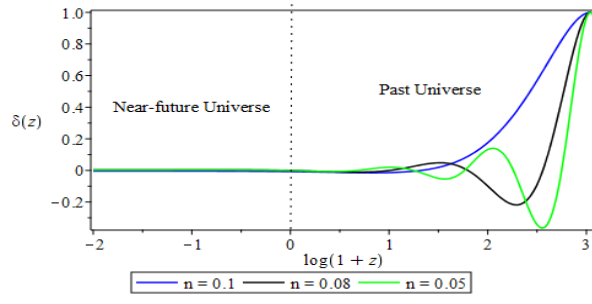


Figure 37: The growth of density fluctuations $\delta(z)$ versus z in long-wavelength mode for Eq. (109) for the values of $n \ll 1$ and for $\Omega_r = 4.48 \times 10^{-5}$.

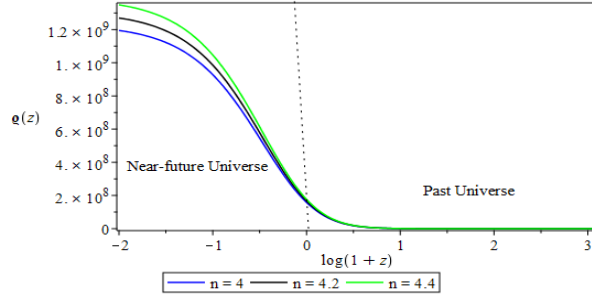


Figure 38: The growth of density contrasts $\varrho(z)$ versus z in long-wavelength mode for Eq. (109) for the values of $n \gg 1$.

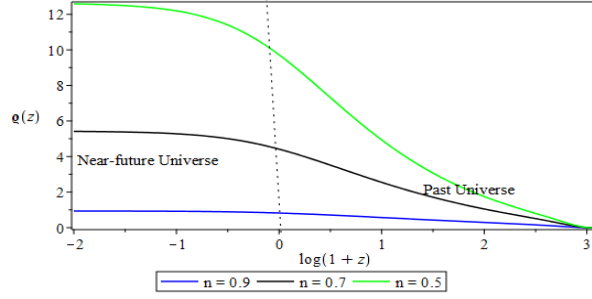


Figure 39: The growth of density contrasts $\varrho(z)$ versus z in long-wavelength mode for Eq. (109) for the values of $0.5 \leq n \leq 1$.

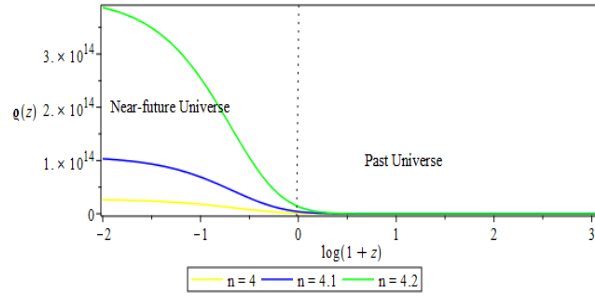


Figure 40: The growth of density fluctuations $\delta(z)$ versus z in long-wavelength mode for Eq. (109) for the values of $n \gg 1$ and $\Omega_r = 4.48 \times 10^{-5}$.

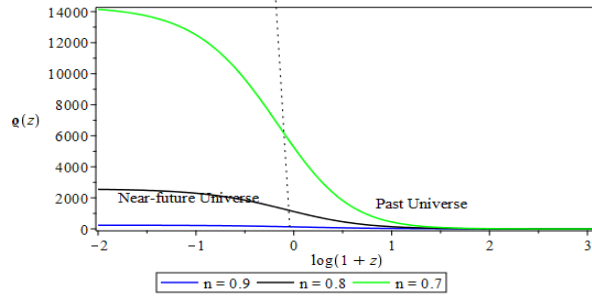


Figure 41: The growth of density fluctuations $\delta(z)$ versus z in long-wavelength mode for Eq. (109) for the values of $n \ll 1$.

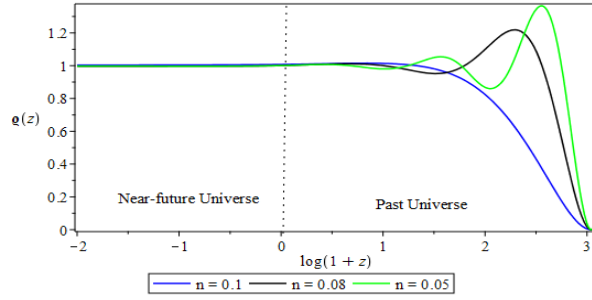


Figure 42: The growth of density fluctuations $\varrho(z)$ versus z in long-wavelength mode for Eq. (109) for the values of n closer to GR.

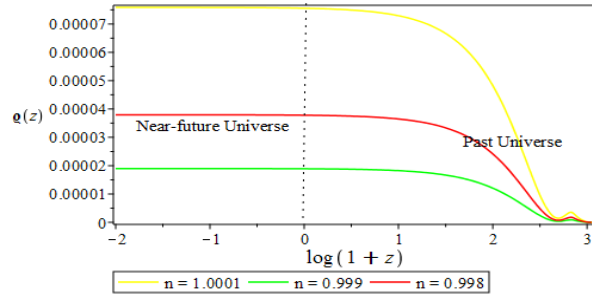


Figure 43: The growth of density fluctuations $\varrho(z)$ versus z in long-wavelength mode for Eq. (109) for the values of n closer to GR and $\Omega_r = 4.48 \times 10^{-5}$.